D2.6 Aviation Climate Change Models

Date: January 31, 2024

Funded by
the European Union

This Project has received funding from the European Union's HORIZON Research and Innovation Programme under Grant Agreement number 101096698

Document Identification			
Status	Final	**Due Date**	31/01/2024
Version	1.0	**Submission Date**	14/03/2024

Related WP	WP2	**Document Reference**	D2.6
Related Deliverable(s)	D3.3, D5.4	**Dissemination Level (*)**	PU
Lead Participant	UC3M	**Lead Author**	Abolfazl Simorgh
Contributors	KTH UoB	**Reviewers**	María Cerezo, UC3M Manuel Soler, UC3M

Keywords:
Environmental Impact; Climate Change Functions; Uncertainty; algorithmic Climate Change Functions; Contrail Cirrus Prediction Model; Kerosene Fuel; Sustainable Aviation Fuel; Aircraft Trajectory Optimization. Air Traffic Management.

Document Information

List of Contributors	
Name	**Partner**
Abolfazl Simorgh	UC3M
María Cerezo	UC3M
Adrián Zarzoso	UC3M
Manuel Soler	UC3M
Evelyn Otero Sola	KTH
Hakki Aksoy	KTH
Simon Blakey	UoB

Document History			
Version	**Date**	**Change editors**	**Changes**
0.1	29/01/2024	Abolfazl Simorgh (UC3M)	Initial draft
0.2	23/02/2024	Abolfazl Simorgh (UC3M)	Improving consistency
1.0	23/02/2024	Abolfazl Simorgh (UC3M)	Final version to be submitted
1.1	11/03/2024	Adrián Zarzoso (UC3M)/ Abolfazl Simorgh (UC3M)	Including reviewers' comments

Quality Control		
Role	**Who (Partner short name)**	**Approval Date**
Deliverable leader	María Cerezo (UC3M)	23/02/2024
Quality manager	Gerardo Zampino (KTH)	14/03/2024
Project Coordinator	Ricardo Vinuesa (KTH)	13/03/2024

Table of Contents

List of Tables

List of Figures

List of Acronyms

Abbreviation / acronym	Description
aCCF	algorithmic Climate Change Functions
AGL	Above Ground Level
API	Application programming interface
ATM	Air Traffic Management
ATR	Average Temperature Response
BFFM2	Boeing Fuel Flow Method 2
CoCiP	Contrail Cirrus Prediction Model
D2.6	Deliverable number 6 belonging to WP 2
EC	European Commission
EEDB	Engine Emission Data Bank
EF	Energy Forcing
EI	Emission Index
EPS	Ensemble Prediction System

F-ATR20	Average Temperature Response Over 20 Years with Future Emissions Scenario
FDR	Flight Data Recorder
FSC	Fuel Sulphur Content
GR	Ground Reference
IAGOS	In-service Aircraft for a Global Observing System
ICAO	International Civil Aviation Organization
ISA	International Standard Atmosphere
ISSR	Ice-SuperSaturated Regions
LHV	Lower Heating Value
LTO	Landing and Take-Off
LW	LongWave
MEEM	Mission Emissions Estimation Methodology
nvPM	Non-volatile Particulate Matter
OLR	Outgoing Longwave Radiation
P-ATR20	Average Temperature Response over 20 years with Pulse Emissions Scenario
PCFA	Persistent Contrail Formation Areas
PMO	Primary Mode Ozone
S2F2	Sustainable Supersonic Fuel Flow Method
SAF	Sustainable Aviation Fuel
SD	Standard Deviation
SN	Smoke Number
SW	Shortwave
TIM	Number of engines
UTLS	Upper Troposphere and Lower Stratosphere
WP	Work Package

Executive Summary

The climate impact of non-CO_2 emissions, accounting for two-thirds of aviation's radiative forcing, is heavily influenced by atmospheric chemistry and weather conditions. Hence, by planning aircraft trajectories to reroute areas where the non-CO_2 climate impacts are strongly enhanced, called climate-sensitive regions, there is a potential to reduce aviation-induced non-CO_2 climate effects. In order to incorporate climate impact in aircraft trajectory planning, there is a need for climate change models that provide detailed spatial and temporal insights into the climate effects of aviation emissions, encompassing future temperature changes at specific times and locations in the atmosphere. Within the EU-Project FlyATM4E, we have developed such models specifically for conventional kerosene fuel. These models called algorithmic climate change functions (aCCFs), utilize key meteorological variables (such as temperature and relative humidity) to calculate the average temperature response (ATR) as a measure of climate impact. However, these aCCFs do not currently apply to sustainable aviation fuels (SAF). In addition, they are deterministic. One of the key challenges in refining these models is addressing multiple factors that introduce uncertainty in climate impact estimates. These include elements such as emissions calculation, weather forecast uncertainties, identification of ice-supersaturated conditions, and the methodologies used to model climate effects. The objective of this deliverable is, therefore, to expand the scope of aCCFs to encompass SAF and its blends with kerosene at varying ratios. In addition, various sources of uncertainty, including weather forecasts, and relative humidity corrections, are considered and will be inputted to flight planning tools. Given the high level of uncertainty in estimating the climate impact of contrails, we also incorporate the Contrails Cirrus Prediction Model (CoCiP) as an alternative method for robust climate change function development. By robust climate change functions, we refer to ensemble estimates of climate impact to characterize uncertainty, a concept similarly used for ensemble prediction system (EPS) weather forecasting. These refined functions will be inputted to WP3, Task 3.3, to develop robust, climate-optimized flight trajectories with minimal sensitivity to uncertainties in climate impact estimates."

2 Introduction

Despite the impacts of the COVID-19 pandemic on the aviation industry during the recent two years, which caused, at European level, declination of 55% and 44% of flight movements in 2020 and 2021, respectively, compared to 2019 [1], it is estimated that the aviation industry will completely recover by 2024 (105% of 2019 at European level) [2] and continue to grow by 1.2% annually. This will require the daily accommodation of 43.7 thousand flights (most-likely scenario) by 2050, which is 44% higher than in 2019 [1]. Such a growth rate of air traffic, in addition to critical operational-related issues such as capacity, efficiency, and safety, will significantly impact the environment within the current air traffic management (ATM) system. Particularly, air traffic operations contribute to climate change through the emissions of CO_2 and other non-CO_2 climate effect [3]. The non-CO_2 climate impact includes changes in ozone and methane concentrations induced by nitrogen oxides (NO_x), water vapor (H_2O), hydrocarbons (HC), carbon monoxide (CO), sulfur oxides (SO_x), and increased cloudiness due to persistent contrail formation [3].

The temperature perturbation resulting from CO_2 emissions is only dependent on the amount of emitted CO_2 due to the long atmospheric lifetime of CO_2. Contrarily, non-CO2 effects occur over short timescales, which typically range from hours (e.g., contrails) to months or years (e.g., NO_x-induced changes on O_3 and CH_4). As a consequence, the temperature perturbation caused by an aircraft unit emission is highly dependent on the time and location of the emission [4]. By taking into account such a spatiotemporal dependencie of non-CO_2 effects in aircraft trajectory planning, it is possible to mitigate their corresponding climate effects. Interested readers are referred to the survey on recent studies in this field (see [5]).

Despite promising potential to reduce climate effects, climate-aware flight planning comes at the cost of increased fuel burn, longer flights, or reduced airspace capacity. Consequently, in addition to measures for avoiding climate-sensitive areas in the first place, the next best strategy, along with the operational measure, might be designed-based strategies that can act as an interim solution together [6]. The use of sustainable aviation fuel (SAF) is considered one of the solutions to reach the aviation industry's commitment to achieving net zero CO_2 emissions by 2050 [7]. The CO_2 is absorbed during their production process with SAFs, meaning that CO_2 emissions on a net basis are reduced and could even hit zero with the correct production and operational processes. SAFs also have a reduced non-CO_2 footprint compared to conventional jet fuels [8]. Their higher purity cuts soot emissions, in turn reducing contrail formation and aviation-induced cloudiness. The RefMAP project

aims, among other objectives, to deliver environmentally optimal air traffic operations through flight planning with conventional fossil fuel, SAFs, and different blending of SAFs.

2.1 Purpose of the document

Due to the dependency of aviation-induced environmental impact on the time and location of emissions, flight planning is known as one of the best strategies to mitigate their corresponding impacts. To optimize aircraft trajectories, we need models that can represent the spatiotemporal dependency of aviation-induced climate effects in order to be included in the objective function of the aircraft trajectory planning problem.

The main objective of the deliverable is, therefore, to provide mathematical models capable of assessing the climate impact of individual species (e.g., contrails and NO_x emissions) for conventional kerosene fuel, SAF, and SAF blended with kerosene with different blending ratios. We will refer to these models as climate change functions throughout the document.

2.2 Relation to other project work

To achieve goals related to aircraft trajectories with minimum environmental impact set in RefMAP, models representing climate impact, noise, and local air quality are required. These models will be considered within the aircraft trajectory optimization to deliver environmental optimal routes from individual flight perspectives (called trajectory-level or micro-level). These independently (i.e., from other flights) optimized trajectories will be integrated into Air Traffic Management (ATM) network-level analysis in order to assess their operational feasibility. If needed, resolution strategies will be performed at this level (called network-level or macro-level) in order to deliver environmentally optimized trajectories feasible from the ATM perspective. The workflow is illustrated in in Figure 1.

Figure 1. Workflow showing relations between tasks related to this deliverable.

This deliverable is within the WP2, related to Task 2.6, i.e., aviation climate change models. The output of this task, jointly with the output of Tasks 2.4 and 4.1, will be inputted to WP3, Task 3.3 for determining environmental-optimal routes from micro-level perspective, which is then required for WP5, Task 5.3 for network-scale analysis.

2.3 Structure of the document

The aim of this deliverable is to present climate change models that will be used for climate-optimal flight planning. These models, presented in Section 3, estimate climate impact in temperature change or energy forcing per emitted species (or distance flown in persistent contrail formation areas in terms of contrail). Therefore, in order to represent climate effects in temperature change or energy forcing, aircraft emissions (e.g., NO_x emissions) along the trajectory need to be calculated. The calculation of emissions, which plays a crucial role in adapting the climate change functions (initially developed for kerosene fuel) to sustainable aviation fuel, will be presented in Section 4. As the climate change functions require meteorological weather data for climate impact estimation, they can be affected by uncertainty in the weather forecast. In addition, the climate impact modeling approach, identification of ice-supersaturate regions, and the assumptions used to calculate emissions of SAF can introduce uncertainty to the climate impact estimates and, in turn, efficiency of the planned trajectories. Therefore, there is a need to provide climate change functions by considering potential uncertainty effects, enabling the determination of more reliable climate-optimized trajectories. Such a modeling approach, which we refer to as robust climate change functions, will be presented and discussed in Section 5. The structure of the document can be graphically seen in Figure 2.

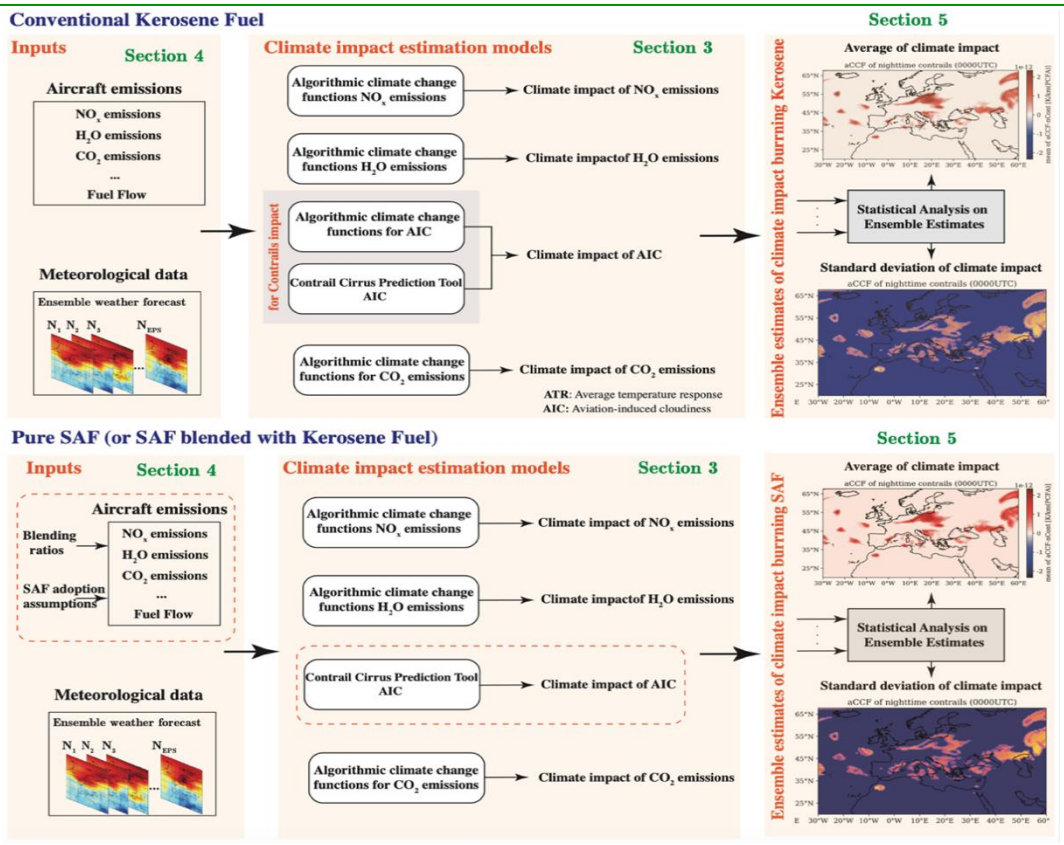

Figure 2. Structure of the document.

3 Climate Change Models

To plan climate-optimal trajectories, spatially resolved information on aviation-induced climate effects is required. Such information are represented as mathematical models in order to include in the objective function of the flight planning problem. In literature, the studies have primarily centered around the use of kerosene as a fuel source to develop climate change models (see Simorgh et al., 2022 for a review). One of the state-of-the-art approaches to model the aviation-induced non-CO_2 effects is toward using the prototype algorithmic climate change (aCCFs) functions which were initially introduced within the EU-project ATM4E and improved within the EU-project FlyATM4E [9], [10]. These aCCFs quantify the climate impact of ozone and methane resulting from NO_x emissions, water vapor emissions, and persistent contrails by taking specific meteorological variables as inputs computationally fast; thus, they are suitable to be employed by aircraft trajectory optimization techniques. We have recently developed an open-source python library

(called CLIMaCCF), implementing the latest version of aCCFs[1] (see Figure 3). The other state-of-the approach is the Contrail Cirrus Prediction Model (CoCiP), which is used to quantify the climate effects of contrails [11]. CoCiP also requires specific meteorological variables, including temperature, specific humidity, top net solar radiation, and top net thermal radiation, and estimates the depth and age of contrails as well as corresponding climate impact in energy forcing. An open-source python library, called pycontrails[2], has been recently released, implementing the CoCiP model.

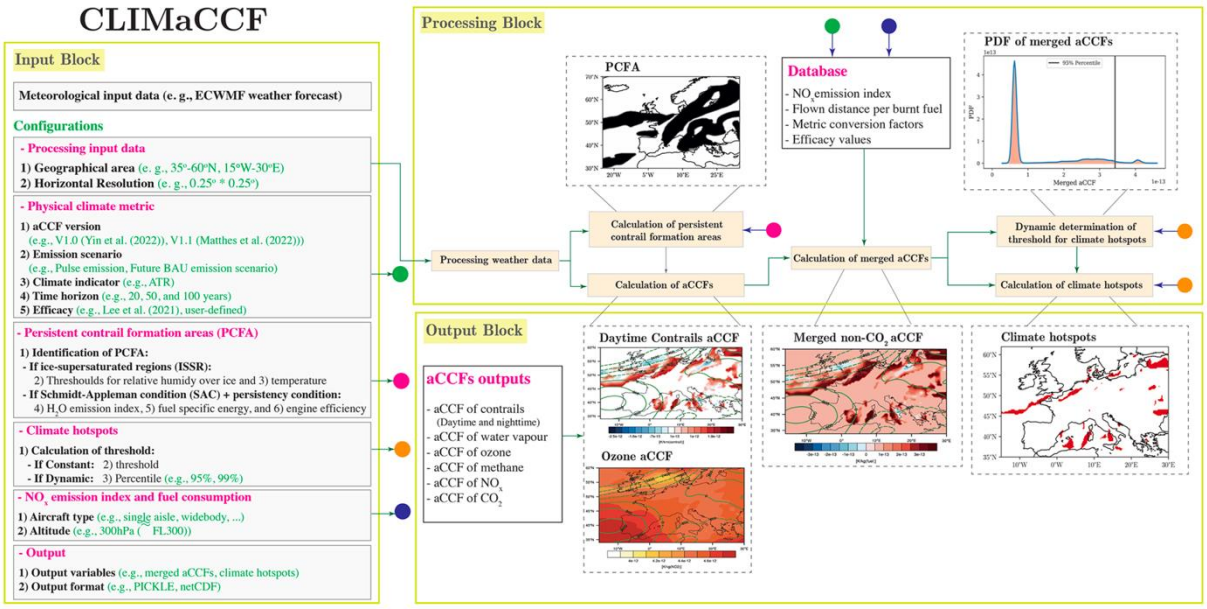

Figure 3. Schematic workflow of calculating individual and merged aCCFs using the Python library CLIMaCCF version 1.0. The left box describes the input block, the upper right box the processing block, and the lower left box the output block.

3.1 Algorithmic Climate Change Functions (aCCFs)

Algorithmic climate change functions are mathematical formulas, which require local meteorological conditions as input and provide, as output, the estimated average temperature response (as the climate indicator), in Kelvins, over the next 20 years (as the time horizon) per kilogram of fuel burnt (in case of CO_2 and H_2O), NO_x emissions (in case of NO_x-induced changes in the atmospheric concentration of

[1] CLIMaCCF library can be accessed using DOI: 10.5281/zenodo.6977272

[2] pycontrails library can be accessed using DOI: 10.5281/zenodo.7877538

ozone and methane), or distance flown in areas favorable for the formation of persistent contrails (in case of contrails) [10]. The aCCF are based on Climate Change Functions (CCFs), which were calculated using a global chemistry-climate model system. Because of their high computational cost, the CCFs were computed only for eight representative weather patterns in winter (five days) and summer (three days) [4]. The aCCFs were developed to identify a correlation between local atmospheric fields and CCFs values, thus allowing calculate ATR20 values for a larger number of background atmospheric conditions, which is needed to solve trajectory optimization problems. The suitability of aCCFs for climate-optimal trajectory planning can be justified as follows:

- aCCFs account for the temporal and spatial dependency of climate impacts associated with non-CO_2 species, including ozone and methane, resulting from NO_x emissions, water vapor emissions, and persistent contrails.
- aCCFs estimate the climate impact associated with aircraft emissions computationally in real time, making it well-suited for climate-optimal trajectory planning.
- aCCFs directly quantify climate impacts in average temperature change.

In the following, general formulations of aCCFs are provided. Note that the formulations show the relation of climate effects of individual species to the relevant meteorological variables, and depending on the version of aCCFs, emission scenario, and time horizon, the parameters $\kappa_{(\cdot)}$ are selected [9].

3.1.1 aCCF of CO_2

The temperature perturbation resulting from CO_2 emissions is only dependent on the amount of emitted CO_2, due to the long atmospheric lifetime of CO_2. Therefore, its climate impact is represented by a constant factor.

$$\text{aCCF}_{CO_2} = \kappa_{16} \quad \text{[K/Kg(fuel)]}$$

which is independent of time, geographical location, and altitude of the emission. The constant factor is determined based on the selected metric.

3.1.2 aCCF of water vapor

Water vapor emissions directly lead to radiative forcing through increased into concentrations in the atmosphere. The lifetime of emitted water vapor depends strongly on altitude and varies between hours and months. The warming climate

impact of water vapor in terms of ATR is modeled using potential vorticity (PV) in $[10^{-6}\mathrm{K}\cdot\mathrm{m}^2/\mathrm{kg}\cdot\mathrm{s}]$ as:

$$\mathrm{aCCF}_{\mathrm{H_2O}} = \kappa_{31} + \kappa_{32}|PV| \quad [\mathrm{K/Kg(fuel)}].$$

3.1.3 aCCF of NO_x emissions

Emitted NO_x has a negligible direct climate impact but leads to a short-term increase in ozone production rates (thus positive radiative forcing) and a long-term increase in methane oxidation (thus negative radiative forcing). Significant seasonal and spatial variability exists in the size and lifetime of perturbations caused by NO_x emissions, mainly due to differing background chemical concentrations and insolation. In the following, the weather-dependent formulations of NO_x-induced ozone and methane climate effects are provided:

3.1.3.1 aCCF of Ozone

The warming effect of ozone resulted from NO_x emissions is captured using local temperature (T) in [K] and geopotential (GH) in $[\mathrm{m}^2/\mathrm{s}^2]$ with the following relation:

$$\mathrm{aCCF}_{\mathrm{O_3}} = \kappa_{11} + \kappa_{12}\cdot T + \kappa_{13}\cdot \mathrm{GH} + \kappa_{14}\cdot T\cdot \mathrm{GH} \quad [\mathrm{K/Kg(NO_2)}]$$

where the weather variables T and GH, and thus the calculated $\mathrm{aCCF}_{\mathrm{O_3}}$, are functions of atmospheric locations at time t, e.g., $T = T$(time, flight level, latitude, longitude). If $\mathrm{aCCF}_{\mathrm{O_3}}$ generates negative values, it is assigned to zero, implying that ozone increase caused by NO_x emissions has a warming effect.

3.1.3.2 aCCF of Methane

Decrease in the methane's concentration from NO_x emissions has a cooling effect. The geopotential and incoming solar radiation at the top of the atmosphere (F_{in}) in $[\mathrm{W/m}^2]$ are found as representative atmospheric variables to quantify the methane's cooling effect with the following relation:

$$\mathrm{aCCF}_{\mathrm{CH_4}} = \kappa_{21} + \kappa_{22}\cdot \mathrm{GH} + \kappa_{23}\cdot F_{in} + \kappa_{24}\cdot F_{in}\cdot \mathrm{GH} \quad [\mathrm{K/Kg(NO_2)}]$$

which is assigned to zero for positive values. Generally, the cooling effects are less strong when compared to the warming effects of ozone. Therefore, the overall climate impact of NO_x emissions is expected to be warming.

3.1.4 aCCF of Contrails

During the day, contrails can cause a cooling effect by reflecting incoming shortwave (SW) solar radiation back to space while trapping and re-emitting longwave (LW)

infrared radiation back to the Earth's surface. While the globally averaged contribution of air traffic to anthropogenic climate forcing is ≈ 3.5%, the regional fingerprint of contrail cirrus on the atmospheric energy budget can be significantly higher. For example, in major air traffic corridors over the United States and Europe, contrail cirrus may warm the atmospheric column by more than 500 mWm^{-2}, and hence contribute substantially to the regional anthropogenic radiative forcing [6], [11].

The aCCF for contrails in [K/km(contrail)] is developed separately for day and night times because its overall climate impact is greatly affected by the emission time.

3.1.4.1 Daytime contrail

The climate effect of contrails during daytime is estimated based on outgoing longwave radiation (OLR) in [W/m^2] with the following relation:

$$\text{aCCF}_{\text{dCont.}} = \kappa_{41}(\kappa_{42} + \kappa_{43} \cdot OLR) \quad \text{[K/km(contrails)]}$$

which can have both cooling and warming impacts.

3.1.4.2 Nighttime contrail

The local temperature with the relation given in provides a good approximation for capturing the climate impact of contrails during the night-time:

$$\text{aCCF}_{\text{nCont.}} = \kappa_{51}(\kappa_{52} \cdot 10^{\kappa_{53} \cdot T} - \kappa_{54}) \quad \text{[K/km(contrails)]}$$

which is assigned to zero for negative values, thus has only warming impact.

Only in areas where persistent contrails are formed the contrails' aCCF will be non-zero and expressed in units of [K/km (distance flown)]. To identify such areas, the ice-supersaturation is applied using temperature and relative humidity over ice, as well as Schmidt-Appleman criterion in order to predict regions where persistent contrails are expected to form, called persistent contrail formation areas (PCFAs) [12].

Metric Conversion and forcing efficacy

As mentioned earlier, values of parameters $\kappa_{(\cdot)}$ depend on the used climate indicator, time horizon, emission scenario, and forcing efficacy (see Dietmüller et al. 2022 for a detailed explanation). In the following, we briefly discuss metric conversion and forcing efficacies.

- **Metric conversion:**

The selection of a suitable metric depends on the question to be answered (see [13] for more details); therefore, different questions require the use of different metrics. The P-ATR20 metric was selected as a metric for the aCCFs to assess the impact of a "simple" pulse emission. However, factors are available (see Dietmüller et al., 2023) to convert P-ATR20 to other metrics: for example, assuming the future emission scenario or longer time horizons. This way, one can select the emission scenario and time horizon that are best suited for the question. In RefMAP project, the F-ATR20 metric is used to assess the climate effect reduction obtained by steadily applying a specific routing strategy under the assumption of a future business-as-usual emission scenario. It is worth mentioning that the conversion factors were derived by simulations with the climate response model AirClim [14]: e.g., one simulation with pulse emission and one with the future emission scenario. By comparing the two simulations, the factors can be derived.

- **Forcing efficacy:**

  Efficacies were introduced to take into account the fact that the radiative forcing of some non-CO_2 forcing agents (e.g., ozone, methane, contrails) is more or less effective in changing the global mean near-surface temperature per unit forcing compared to the response of CO_2 forcing [15]. have summarized the efficacy parameters reported by Lee et al., 2021. For a detailed explanation of efficacy, the reader is referred to the state-of-the-art literature (e.g., Ponater et al., 2006 [15], Rap et al., 2010 [16], Bickel et al., 2020 [17]).

In RefMAP, the parameters $\kappa_{(\cdot)}$ are selected to represent the climate effects using the future emission scenario, 20-year time horizon, and efficacy parameters reported by [3]. The first version of the CLIMaCCF library enables users to specify the version of aCCFs, efficacy parameters, emission scenario, and time-horizon in the configuration file (see Figure 3).

The fuel consumption, NO_x emissions, and distance flown in persistent contrail formation areas are required to quantify the climate effects in Kelvin.

Analysis of aCCFs for specific meteorological condition

As an application example, we show typical winter patterns of water vapor, NO_x-induced (including ozone, methane, and primary mode ozone (PMO)), contrail-cirrus, and merged non-CO_2 aCCFs at 0000 UTC (under nighttime conditions) on the 1st of January 2023 over the geographical region of Europe (15° W–30° E, 35–60° N) at a pressure level of 250 hPa. With this analysis we aim to give an impression of the

typical structure and of gradients of the specific aCCFs over the European airspace. Note that, we generated individual and merged aCCFs using aCCF-V1.0A and by assuming the climate metric of F-ATR20 with inclusion of efficacies. To generate the merged aCCFs and to compare the contribution of each species, we adopt typical transatlantic fleet mean values to unify the units of aCCFs in K/kg(fuel). The approximated conversion factors for NO_x emissions and contrails are 0.013 kg(NO_2)/kg(fuel) and 0.16 km/Kg(Fuel), respectively [18], [19]. In the case of merged aCCFs, we will focus on the merged non-CO_2 aCCFs, as the merged aCCF pattern does not change if including the CO_2 aCCF, which has a constant value in time and location.

The meteorological variables required for calculating aCCFs are depicted in Figure 4. The geographical aCCF patterns of water vapor, NOx emissions, contrail (daytime and nighttime), merged non-CO_2, and persistent contrail formation areas are shown in Figure 5. As aircraft-induced water vapor emissions have a warming effect, the water vapor aCCFs reveal positive values in all regions. The values of water vapor aCCF are highly variable, and they vary with location by a factor of about 3. This regional variation in the aCCFs pattern highly follows the weather pattern (i.e., potential vorticity).

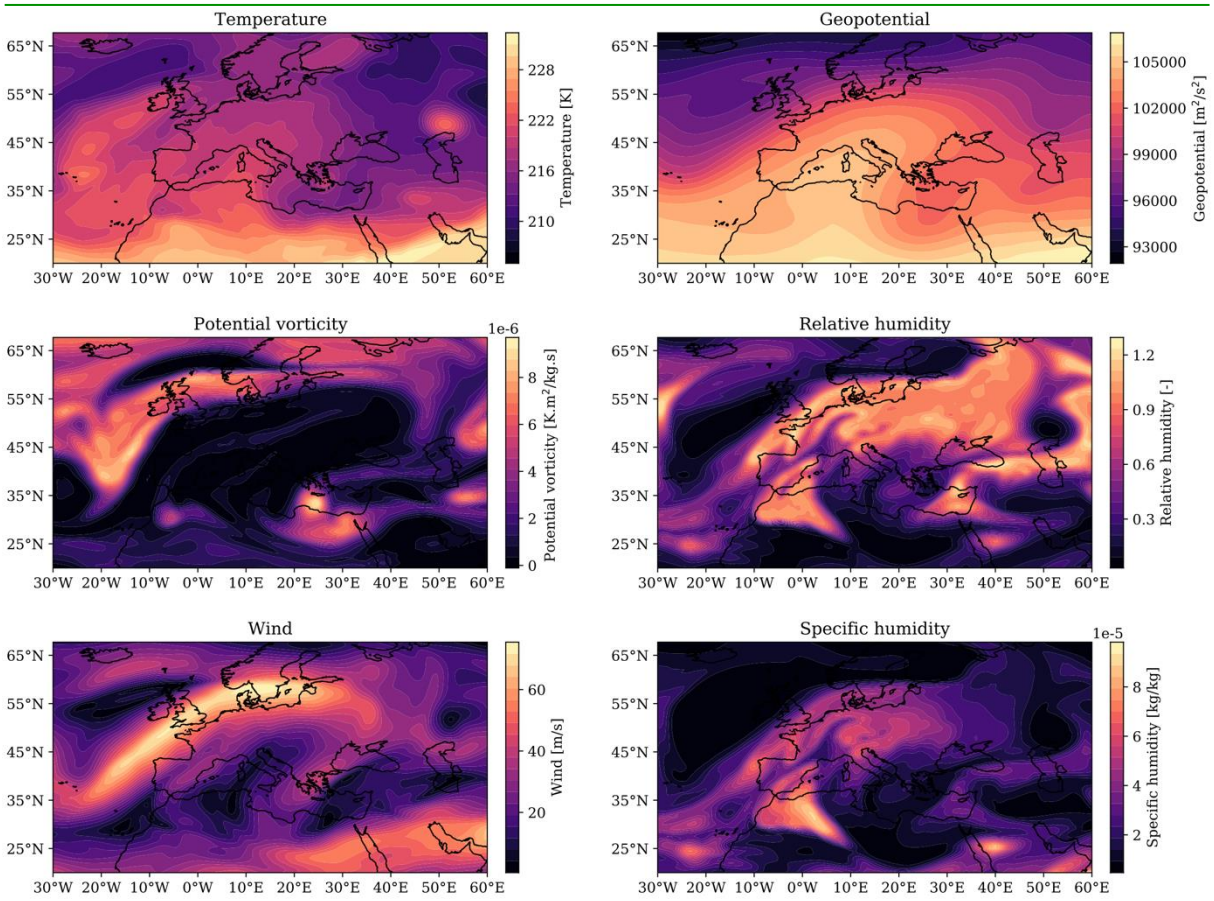

Figure 4. Meteorological variables required to calculate non-CO_2 climate effects on 1st of January 2023, over European airspace at 250hPa.

To better understand the total NOx-induced aCCF, the NO_x aCCF is displayed in Figure 5 together with the ozone and methane aCCF. Note that the long-term primary-mode ozone (PMO) is included here in the methane aCCF. The ozone aCCF is positive (warming), as NO_x emissions from aviation induce the production of the greenhouse gas ozone. It reveals generally higher values in southern regions, as photochemical ozone formation increases with the availability of sunlight as well as with temperature. Additionally, the synoptical weather pattern influences the ozone aCCF values, as emitted NOx that is transported to lower latitudes experiences more solar radiation, and thus photochemical ozone production is higher compared to that which remains at higher latitudes. The methane aCCF is negative, as NO_x emissions cause a decrease in methane concentrations, as there is a decrease in warming from methane. The resulting total NO_x aCCF, a combination of ozone warming and methane net cooling effects, reveals that the ozone effect dominates the overall warming effect of NO_x emissions. Note that by using the metric of ATR20 and an underlying future emission scenario, the differences in lifetime between NO_x, ozone, and methane are taken into account.

Only if the atmospheric conditions allow for a contrail formation (which we refer to as persistent contrail forming areas) is the contrail aCCF nonzero. Figure 5 shows daytime and nighttime contrail-cirrus aCCFs that can lead to either a positive or negative climate effect. During daytime, whether the climate effect is positive or negative depends mainly on the solar insolation, as contrails not only reduce the outgoing longwave radiation (warming) but also reflect the shortwave incoming radiation (cooling). The spatial variability in the contrail aCCF is very high and ranges from zero (regions with no persistent contrail formation) to high positive or negative values. This is clear as the formation of persistent contrails is highly sensitive to the actual atmospheric conditions. Regarding the merged non-CO_2 aCCF, the contrails have dominant climate effects, which is in line with related studies employing aCCFs (e.g., see [9]. Based on the merged aCCF, a hypothetical climate-optimized European flight (which will stay on this pressure level for simplification) would certainly try to avoid the areas with high positive merged aCCFs. Further, this flight trajectory will probably find a compromise between avoiding long distances through enhanced climate warming areas and at the same time avoiding long detours as these would induce a penalty with respect to CO_2 aCCF. Thus, if the trajectory is optimized based on the merged non-CO_2 aCCF, this penalty is not considered.

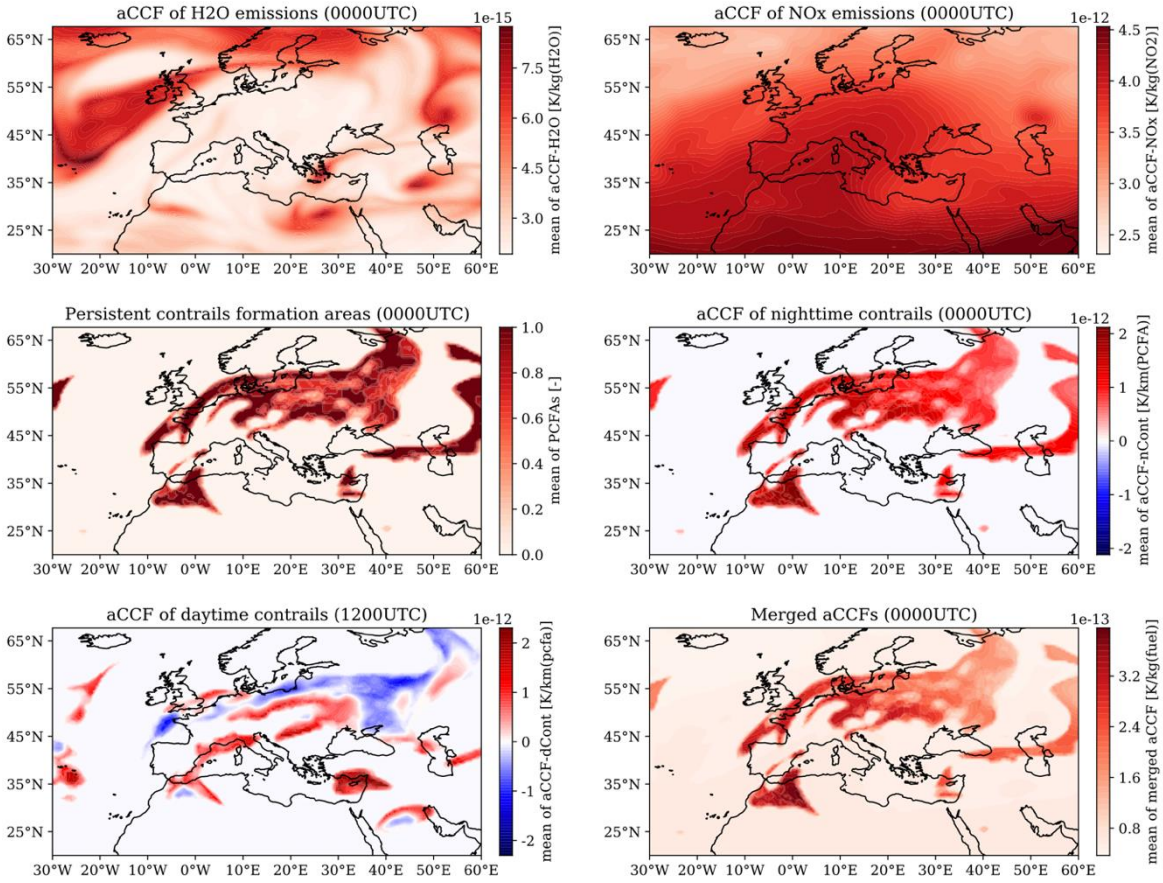

Figure 5. Algorithmic climate change functions of water vapor, NO_x emissions, contrails, and the merged non-CO_2 effects on 1st of January 2023, over European airspace at 250hPa.

3.2 Contrail-cirrus Prediction Model (CoCiP)

The Contrail Cirrus Prediction Model is a tool designed to predict contrail cirrus formations from both individual flights and fleets of cruising aircraft on a regional or global scale. This model is used to calculate the properties (e.g., optical depth) and lifecycle of each contrail, accounting for relevant meteorological factors like wind, temperature, humidity, and ice water content derived from numerical weather prediction outputs, in order to estimate the corresponding energy forcing (EF) as

$$\text{Contrail EF} = \int_0^t RF'(\tau) \cdot L(\tau) \cdot W(\tau) \mathrm{d}\tau$$

where RF′ is the change in energy flux per contrail area, L is the length, W is the width and t is the contrails lifetime. Detailed formulations for estimating climate effects using CoCiP can be found in Schumann, 2012 [11]. CoCiP has been released

as an open-source Python library, called pycontrails with an API[3] for ease of usage. Two possibilities have been provided with the library: the trajectory approach [11] and the grid approach [20]. The trajectory approach involves posting a flight's data to a specific API endpoint, which then calculates the aircraft performance characteristics and energy forcing along the flight trajectory. This method considers the sequence of waypoints, airspeed, fuel flow, and engine efficiency values. On the other hand, the grid approach involves requesting precomputed gridded CoCiP data, which is then interpolated to the trajectory data.

The results of these two methods generally agree in terms of the order of magnitude for total energy forcing, but there can be substantial differences in the outputs, often due to the sensitivity of the initial contrail persistence model to specific ambient conditions. It is important to note that these models assume certain nominal aircraft cruising profiles at each grid point, and the differences between the trajectory and grid models can increase when the actual aircraft performance characteristics deviate from these nominal profiles.

Generally, one can consider the following use cases for these two approaches:

Grid approach use-cases

- Optimization of a flight or fleet for contrail informed flight planning
- Simulation
- Quantify intrinsic model uncertainties through Monte Carlo rollout

Trajectory approach use-cases

- Precise prediction of energy forcing according to latest scientific research published on CoCiP.
- Retrospective / hindcast analysis.

[3] https://py.contrails.org

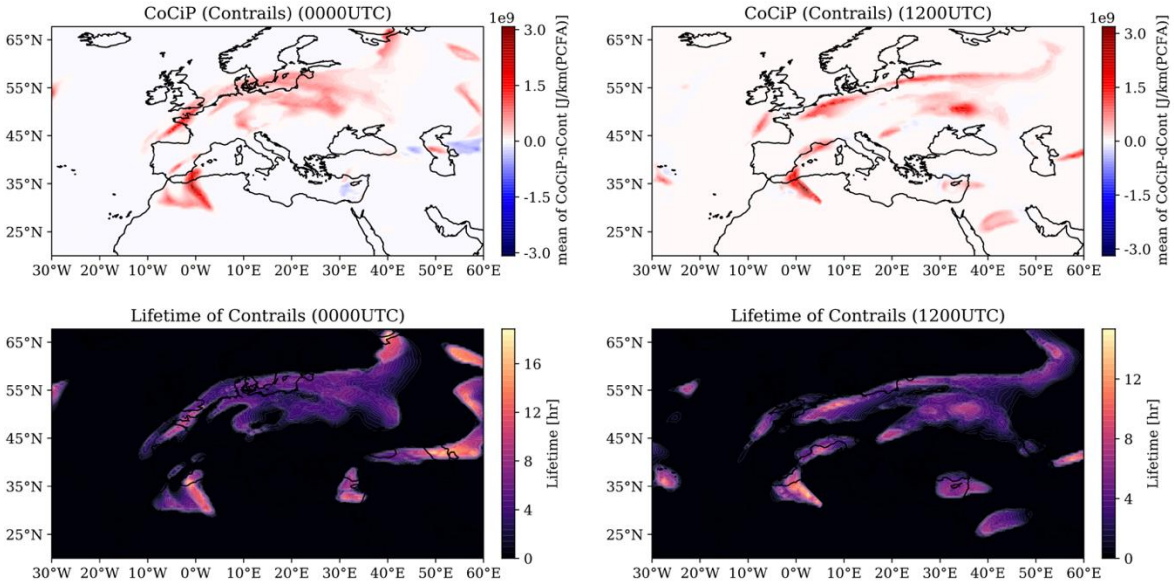

Figure 6. Lifetime and energy forcing of contrails estimated using gridded CoCiP on 1st of January 2023, over European airspace at 250hPa.

Figure 6 illustrates the energy forcing and lifetime of contrails estimated using gridded CoCiP on 1st of January 2023 over European airspace at 250hPa. It can be seen that spatial information on contrails climate sensitivity, similar to aCCFs, is provided with the gridded CoCiP. In addition, the gridded CoCiP provides other properties apart from climate impact, such as the lifetime of contrails. In Figure 6, we see that, for a flight departing at midnight, contrails can persist until 16 hours, leading to a cooling impact in particular areas. The contrails' climate impact estimated using aCCF and gridded CoCiP does not match entirely, and a discrepancy can be seen, which we will discuss in Section 5.

4 Aircraft Emissions Calculation

The climate impacts induced by aviation are initiated by emissions. The climate change functions presented in Section 3 require emissions of specific species in order to quantify climate effects in temperature change (for aCCFs) or energy forcing (for CoCiP). The following presents the approaches utilized in RefMAP to estimate emissions when burning conventional kerosene and sustainable aviation fuel.

The combustion products of the aircraft gas turbine engine are composed of carbon dioxide (CO_2), water vapor (H_2O), unburned hydrocarbons (HC), carbon monoxide (CO), nitrogen oxides (NO_X), excess atmospheric oxygen (O_2) and nitrogen (N_2), and soot [21], [22]. In order to calculate total exhaust emissions during a flight segment,

the emissions index (EI), defined as the mass of pollutant emitted per unit mass of fuel burned for a specified engine, must be calculated for these emissions. CO_2 and H_2O emissions are directly proportional to fuel burned. However, HC, CO, NO_X, and soot are affected by several parameters, such as engine type, power setting, flight altitude, and atmospheric conditions. In the International Civil Aviation Organization's (ICAO) aircraft engine emission data bank (EEDB), emissions of CO, HC, NO_X, non-volatile particulate matter (nvPM) and smoke number (SN), together with associated fuel flow rates, are provided at a set of four reference power settings defined as "take-off", "climb", "approach" and "idle". ICAO EEDB is publicly available at worldwide web[4], and updates to the EEDB are made as new engines are certified. EIs provided in the ICAO EEDB can be directly used to calculate the amount of emissions of CO, HC, NO_X, nvPM mass and nvPM number below the 3000 ft above ground level (AGL).

ICAO EEDB cannot be directly used to calculate the amount of emissions of CO, HC, NO_X, nvPM mass and nvPM number above the 3000 ft AGL. The Boeing Fuel Flow Method 2 (BFFM2)[23] is one of the most widely used methodologies to calculate in-flight emissions of HC, CO, and NO_X, and the mission emissions estimation methodology (MEEM)[24], which is one of the methodologies used to estimate in-flight nvPM emissions are used to calculate the emissions above 3000 ft AGL. Both BFFM2 and MEEM are developed with respect to the conventional kerosene-type fuels and required modifications/extra steps have been detailed in the following sections to calculate the in-flight emissions of sustainable aviation fuels (SAF).

4.1 Calculation of EIs for HC, CO and NO_X

BFFM2 is one of the methodologies used to calculate the emission indices of HC, CO, and NO_X at any flight altitude. Since BFFM2 utilizes the fuel flow parameter of the engine, which can be obtained by simulation or Flight Data Recorder (FDR) data and publicly available EI values from the ICAO EEDB, it is possible to calculate the EI of HC, CO, and NO_X at any flight altitude without the need for any engine proprietary data [23]. The BFFM2 process begins with the correction of the in-flight fuel flow rate to the corresponding sea level fuel flow rate (Equation 1). The corrected fuel flow is then used to obtain the corresponding emission indices of HC, CO, and NOx at sea level, which are used in the final step to calculate emission indices at flight altitude. In the ICAO EEDB, fuel flow rates and emissions indices under the International Standard Atmosphere (ISA) conditions at sea level are given by the engine model for the following flight phases: take-off, climb, approach, and idle. A

[4] https://www.easa.europa.eu/en/domains/environment/icao-aircraft-engine-emissions-databank

correlation between fuel flow rates and emission indices at sea level is established using these four data points in order to calculate the corresponding emission index values for any fuel flow rate. Equations (2) to (4) are used in the last step of the BFFM2 process to correct the obtained sea level emission indices to flight altitude.

$$ff_{sl} = ff_{alt}\frac{\theta_{amb}^{3.8}}{\delta_{amb}} exp^{0.2M^2} \quad (1)$$

$$EIHC_{alt} = EIHC_{sl}\frac{\theta_{amb}^{3.3}}{\delta_{amb}^{1.02}} \quad (2)$$

$$EICO_{alt} = EICO_{sl}\frac{\theta_{amb}^{3.3}}{\delta_{amb}^{1.02}} \quad (3)$$

$$EINO_{X_{alt}} = EINO_{X_{sl}}\sqrt{\frac{\delta_{amb}^{1.02}}{\theta_{amb}^{3.3}}}e^{H} \quad (4)$$

where $\theta_{amb} = \frac{T_{amb}[K]}{288.5}$, $\delta_{amb} = \frac{P_{amb}[Pa]}{101325}$. ff_{sl} is corrected fuel flow at sea level in [kg/s] and ff_{alt} is fuel flow at flight altitude [kg/s]. $EIHC_{sl}, EICO_{sl}$, and $EINO_{X_{sl}}$ are HC, CO, and NO_X emission indices at sea level, and $EIHC_{alt}, EICO_{alt}$, and $EINO_{X_{alt}}$ are HC, CO, and NO_X emission indices at flight altitude, respectively. Finally, the total emissions for a flight segment is calculated using Equation 5:

$$Total\ Emission\ (X) = E_n \cdot EI(X) \cdot TIM \cdot ff_{alt} \quad (5)$$

where E_n, $EI(X)$, and TIM denotes the number of engines, emission index for the pollutant X [g/kg fuel], and time in mode [s], respectively.

4.1.1 Calculation of EIs of HC, CO and NO_x for SAFs

The original BFFM2 was developed with respect to conventional kerosene-type fuels and does not consider the type of fuel used. Therefore, some modifications are needed to calculate altitude emissions when utilizing SAF fuels. Analyzing the BFFM2 application processes shown in Figure 7 reveals that steps 1 and 2 (black number) require modifications. Step 3, which corrects the sea level emission index to the flight altitude and is independent of the used fuel type.

Fusaro et al. [25] modified the original BFFM2 to extend it to supersonic speed regime and different types of fuels. They called the updated method the Sustainable

Supersonic Fuel Flow Method (S2F2). The engine fuel flow rate correction, according to the original BFFM2 method, is derived from the energy balance across the combustor. According to Fusaro et al. [25], the lower heating value (LHV), an energetic index that represents the fuel energy content, or the amount of energy the fuel can release, is the most significant of all the factors of the energy balance through the combustor. Therefore, the LHV property of pure kerosene and kerosene-SAF blend fuels can be used to correct the in-flight fuel flow of pure kerosene fuel. Insight of this knowledge, the fuel flow rate correction developed with reference to conventional kerosene-type fuel can be updated with a coefficient (K_{blend}) derived from the LHV of conventional kerosene-type fuel and LHV of a blend of different fuels:

$$K_{blend} = \frac{LHV_{kerosene}}{LHV_{blend\ \%z}} \tag{6}$$

where z is the percentage of SAF in SAF-kerosene blend, $LHV_{kerosene}$ is the LHV of pure kerosene fuel, and $LHV_{blend\ z\%}$ is the LHV of the SAF-kerosene blend. According to Zschocke et al. [26] and Striebich et al. [27], the LHV of a fuel blend is linear with respect to the blend ratios of fuels. Therefore, $LHV_{blend\ z\%}$ is calculated as[25]:

$$LHV_{blend\ z\%} = \frac{LHV_{100\ \%SAF}\ .\ z + LHV_{kerosene}(100-z)}{100} \tag{7}$$

where $LHV_{100\%SAF}$ is the LHV of the pure SAF. Consequently, the corrected fuel flow rate in original the BFFM2 was modified for SAF blend as:

$$ff_{sl} = ff_{alt} K_{blend} \frac{\theta_{amb}^{3.8}}{\delta_{amb}} e^{0.2M^2} \tag{8}$$

On the other hand, the remaining equations of BFFM2 are left as the original ones since the authors still use the EI of kerosene-type fuel from the ICAO EEDB. We aim to improve the modified BFFM2 developed by Fusaro et al. to estimate the emissions of SAFs at different blending ratios. For that, we consider two approaches: (i) to apply a more precise fuel flow correction factor to kerosene-type fuel, (ii) to modify the sea level EI model of the kerosene fuel by applying a correction factor to EI and fuel flow values of the ICAO databank. The resulting improved model will reduce the error in emissions estimation during flight using SAF.

Each step of the proposed modified BFFM2, aiming to improve the S2F2 methodology developed by Fusaro et al. [25], is depicted in Figure 7. The three main steps of the original BFFM2 are numbered in black color in Figure 7. The proposed

modified BFFM2 consists of 4 steps (numbered in red color), and both fuel flow correction and EI correction are performed at sea level conditions. The first step is the same as the original BFFM2 and correlates the in-flight fuel flow of kerosene-type fuel to sea-level conditions. The second step, detailed in the following, is the fuel flow correction step for the kerosene-SAF blend. The third step is the calculation of EIs for kerosene-SAF blends from the SAF-corrected EI and fuel flow data from ICAO EEDB. The details of how we plan to correct the EIs for kerosene-SAF blends are also provided in the following. The last step is to apply pressure correction to sea level EIs of the kerosene-SAF blend and to apply fuel flow rate correction (inverse of step 1) to the sea level fuel flow of the kerosene-SAF blend in order to calculate corresponding in-flight EIs and fuel flow values of the kerosene-SAF blend.

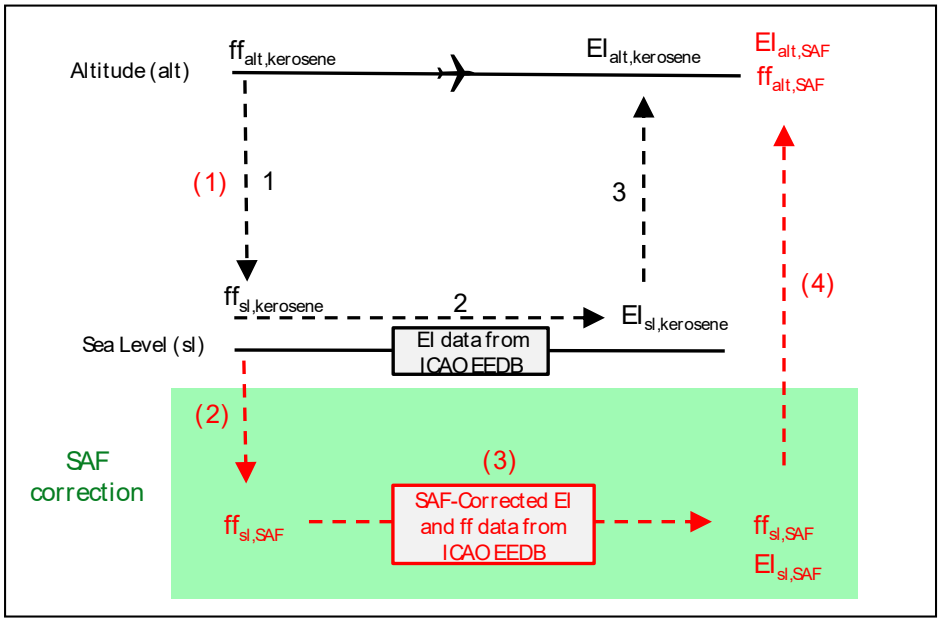

Figure 7 Process of the proposed SAF-modified BFFM2.

Our goal is to more accurately estimate the fuel flow value for kerosene-SAF blends, $ff_{sl,SAF}$ under sea-level conditions when using these blends instead of pure kerosene fuels. When analyzing the energy balance equation provided in the original BFFM2, burner efficiency emerges as another important factor within the energy balance across the combustor. As a part of thermodynamic efficiency, combustion efficiency can be used with the LHV property since several studies, examining the fuel and emission performance of SAFs, have reported significant differences in combustion efficiency for low power settings compared to conventional pure kerosene fuels [28], [29]. Given this information, we decided to redefine the K_{blend}- fuel flow correction factor. Unlike the previous definition established solely as a function of LHV by Fusaro et al.[25], our redefinition incorporates both LHV and combustion efficiency to

enhance its accuracy. We use Equation 9 which computes the combustion efficiency based on the emissions indices of HC and CO [21]:

$$1 - \eta_c = (EI_{HC} + 0.232EI_{CO})10^{-3} \quad (9)$$

The new K_{blend}- fuel flow correction factor is defined as:

$$K_{blend} = k_1 k_2 \quad (10)$$

where

$$k_1 = \frac{LHV_{kerosene}}{LHV_{blend\ z\%}} \qquad k_2 = \frac{\eta_{c,kerosene}}{\eta_{c,blend\ z\%}} \quad (11)$$

Engine emission indices provided in ICAO EEDB for kerosene-type fuel can be used as a reference and we can update these EIs for SAF blends at sea level. In order to update the EIs of kerosene fuel, we aim to calculate emission index correction factors, $E_{blend,HC}$, $E_{blend,CO}$ and $E_{blend,NOx}$ as we did for fuel flow correction. We have planned two approaches to calculate emission index correction factors for the modification of the EIs provided in ICAO EEDB for kerosene-type fuel: (i) benefit from literature data to apply a correction factor to EIs of kerosene-type fuels (ii) perform chemical kinetic modeling of the engine combustion process to estimate EIs of kerosene-SAF blends. At this point, we could not obtain enough data from the literature to obtain a correction factor, but we are about to finalize the chemical kinetic modeling of the engine combustion process to estimate the EIs of kerosene-SAF blends. After obtaining the correction factors to be applied to the EIs of the kerosene-type fuel, the EIs of SAF blends at sea level can be calculated as:

$$EIHC_{sl,blend} = EIHC_{sl,kerosene} E_{blend,HC} \quad (12)$$

$$EICO_{sl,blend} = EICO_{sl,kerosene} E_{blend,CO} \quad (13)$$

$$EINOx_{sl,blend} = EINOx_{sl,kerosene} E_{blend,NOx} \quad (14)$$

4.2 Calculation of EI for Non-Volatile Particulate Matter (nvPM)

The MEEM developed by Ahrens et al.[24] is one of the methodologies used to calculate the non-LTO emissions of nvPM mass (EI_{mass}) and nvPM number (EI_{number}). The method is considered as the synthesis and improved version of the previously

developed methods and is used in a similar manner as BFFM2. The method relies on the LTO nvPM emissions data from the ICAO EEDB, but also allows for previously certified engines which do not have data in the EEDB. For these previously certified engines that do not have nvPM LTO data in EEDB, the nvPM emission indices are estimated from their smoke number certification values using the SCOPE11 correlative methodology developed by Agarwal et al. [30], described in Step 0 of the MEEM method. The MEEM method consists of five main steps, and a flowchart is given in Figure 8.

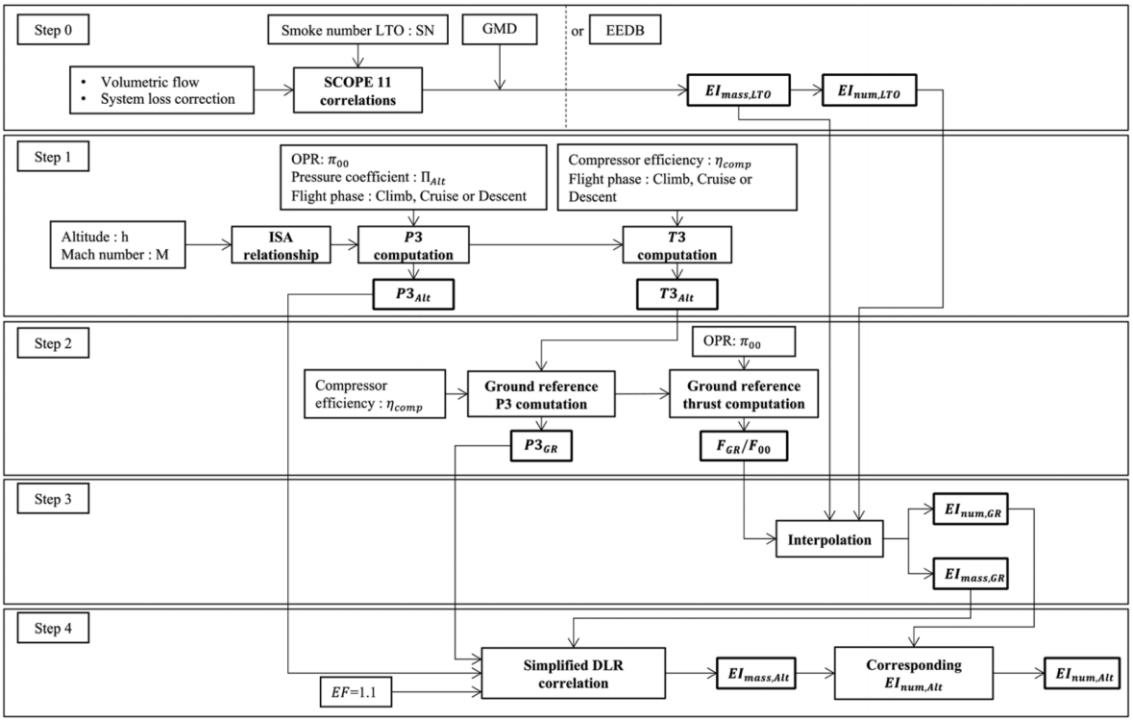

Figure 8 The flow chart of MEEM method [24].

Step 0 of the MEEM is used for engines that their nvPM data is available in the EEDB. It allows calculating the EI_{mass} and EI_{num} from smoke number data for the four LTO conditions. Step 1 consists of estimating the temperature and pressure outside the engine and inside the combustion chamber for the flight conditions related to each segment. Based on these Step 1 estimations, a corresponding ground reference (GR) state is selected. GR thermodynamics properties are calculated through Step 2. The values of nvPM EIs are only available at the four LTO conditions, hence not for an arbitrary GR condition. Step 3 introduces an interpolation method to estimate nvPM EIs at any specific GR condition. Finally, Step 4 facilitates the computation of in-flight nvPM emissions by employing a ground-to-flight transposition correlation.

4.3 Calculation of EI of nvPM for SAFs

Emissions of nvPM for SAFs can be calculated by the combination of MEEM and methodology proposed by Teoh et al.[31]. In MEEM, corresponding EI_{mass} and EI_{number} at sea level are estimated by using the ratio of calculated GR thrust and the nominally rated thrust of the engine (F_{GR}/F_{∞}). The fuel to be used instead of kerosene-type fuel must be 'drop in'. In other words, pure SAF or SAF blends should be able to replace kerosene fuel in a manner that does not require modification of the aircraft/engine fuel systems or result in different engine performance[25], [32], [33]. Therefore, if the change in EI_{mass} and EI_{number} at sea level are estimated in the case of using SAF, we can still use the same ratio of (F_{GR}/F_{∞}) to estimate corresponding nvPM emission indices.

The methodology proposed by Teoh et al.[31] can be used to estimate the change in EI_{number} in the case of using SAFs instead of kerosene fuels. The proposed methodology is based on the difference in hydrogen mass content between the reference fuel and SAF (ΔH), and the ratio of calculated GR thrust and the nominally rated thrust of the engine defined as $\hat{F} = \left(\frac{F_{GR}}{F_{\infty}}\right)$. ΔEI_{number} is estimated from the formula given as:

$$\Delta EI_{number}(\%) = \begin{cases} \left(-114.21 + 1.06\hat{F}\right)\Delta H & ,when\ \Delta H \leq 0.5\% \\ \left(-114.21 + 1.06\hat{F}\right)\Delta H \cdot e^{(0.5-\Delta H)} & ,when\ \Delta H > 0.5\% \end{cases} \quad (15)$$

4.4 Calculation of Fuel Properties and EIs Proportional to Fuel Consumed

The prediction of emissions for SAF fuel blends from the EEDB requires knowledge of the hydrogen content, calorific value, and Sulfur content of the conventional fossil-derived fuel and the SAF product, which are blended together. For newer engine cases in the EEDB, where nvPM emissions tests are carried out at the same time as gaseous emissions, sufficient information is available to determine these fuel properties from the EEDB worksheet named "nvPM Emissions". However, if the nvPM measurements are not made at the same time as the reported gaseous emissions data in the EEDB, then it is not possible to extract these values from the EEDB as they are not reported in the same way for the ICAO engine certification for gaseous emissions. In such cases, an alternative approach to estimate the missing fuel properties is proposed, using average values for these key properties taken from available fuel property surveys.

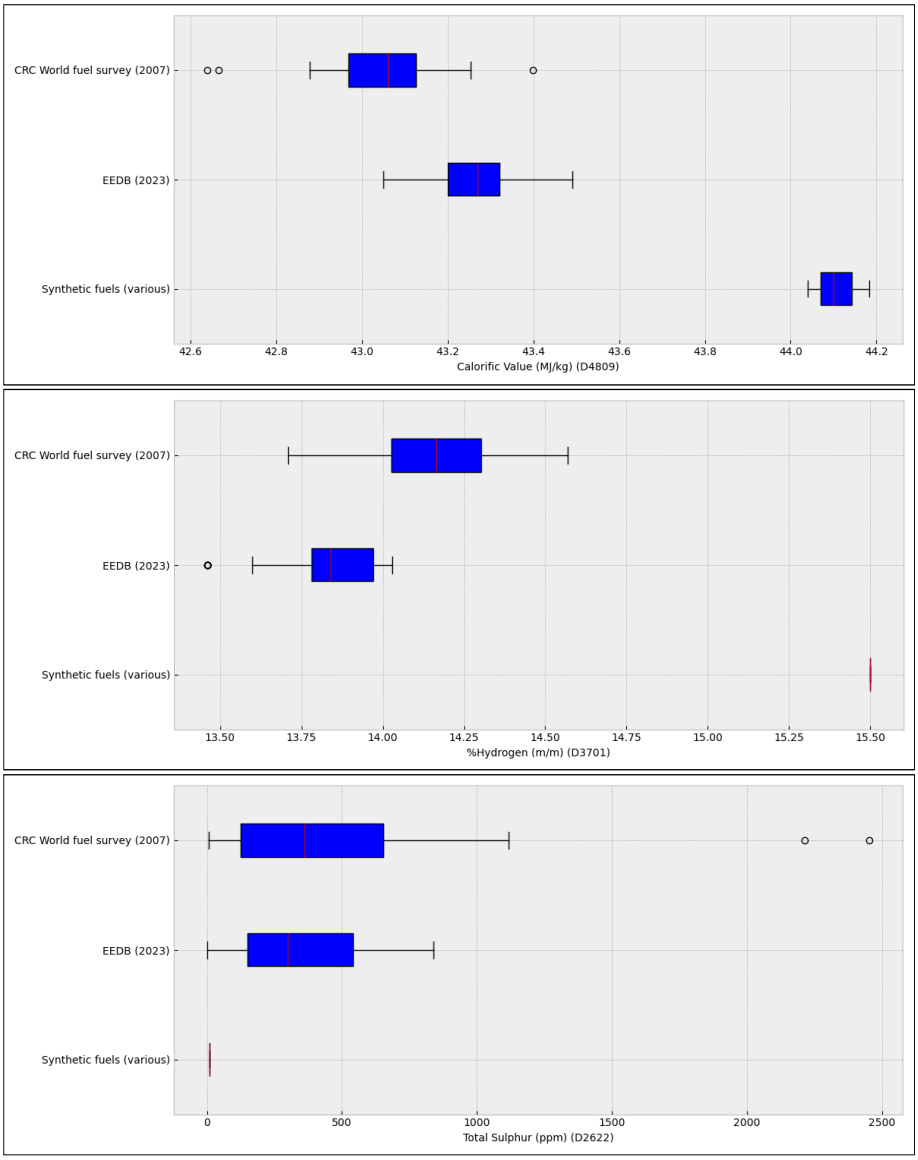

Figure 9 Average properties chart for conventional fuels and synthetic fuels [34].

4.4.1 Calculation of Lower Heating Value of SAF Blends

Several studies in the literature reported that the LHV of a fuel blend is linear with respect to the blend ratios of neat fuels [26], [27], [35], [36]. Therefore, the lower heating value of a blend is calculated as the following:

$$LHV_{blend} = \sum_i w_i \cdot LHV_i \quad (16)$$

where LHV_{blend} is the lower heating value of the blend, w_i is the weight fraction of the neat blend component, and LHV_i is the lower heating value of the neat blend component.

4.4.2 Calculation of Hydrogen Content of SAF Blends

Several studies in the literature reported that the hydrogen content (*H)* of a fuel blend linearly depends on the blend ratios of neat fuels [27], [35], [36]:

$$H_{blend} = \sum_i w_i \cdot H_i \ , \tag{17}$$

where H_{blend} is the hydrogen content of the blend, w_i is the weight fraction of the neat blend component, and H_i is the hydrogen content of the neat blend component.

4.4.3 Calculation of EI for H_2O

The assumption that all the hydrogen in the fuel has been converted to water vapor (H_2O) does not take into account the combustion efficiency of the combustor and fuel combination at the flight conditions concerned. Under real combustion conditions, there is always an emission of HCs. By incorporating a correction factor based on the hydrogen content of the blended fuel and the fuel used in the ICAO emissions database and a factor based on combustion efficiency, as defined in Equation 9, a more accurate estimation of water vapor emission can be made as:

$$EI_{H_2O,blend}\left(\frac{g}{kg}\right) = EI_{H_2O,kerosene}\frac{H_{blend}}{H_{kerosene}}\frac{\eta_{c,blend}}{\eta_{c,kerosene}} \ . \tag{18}$$

4.4.4 Calculation of EI for CO_2

The assumption that all the carbon in the fuel has been converted to carbon dioxide does not take into account the combustion efficiency of the combustor and fuel combination at the flight conditions concerned. Under real combustion conditions, there is always an emission of CO and HCs. By incorporating a correction factor based on the carbon content of the blended fuel and the fuel used in the ICAO emissions database and a factor based on combustion efficiency, as defined in Equation 9, a more accurate estimation of carbon dioxide emission can be made as:

$$EI_{CO_2,blend}\left(\frac{g}{kg}\right) = EI_{CO_2,kerosene}\frac{C_{blend}}{C_{kerosene}}\frac{\eta_{c,blend}}{\eta_{c,kerosene}} \ , \tag{19}$$

or

$$EI_{CO_2,blend}\left(\frac{g}{kg}\right) = EI_{CO_2,kerosene}\frac{100 - H_{blend}}{100 - H_{kerosene}}\frac{\eta_{c,blend}}{\eta_{c,kerosene}} . \quad (20)$$

To determine the carbon content of kerosene, we can apply the principle of conservation of mass and utilize the known mass fraction of hydrogen present in the fuel. Assuming kerosene comprises only carbon and hydrogen, we calculate the weight percent carbon by subtracting the weight percent hydrogen from 100%. This method ensures the total equals 100%.

4.4.5 Calculation of EI for Sulfur Dioxide (SO_2) and Sulfate (SO_4^{2-})

Sulfur contained in the fuels burned by aircraft engines emerges as the source of both SO_2 and Sulfate emissions. Fuel sulfur is first oxidized in the combustor of jet engines, and it is released at the engine's exit plane primarily as SO_2. Sulphate is formed from the fuel sulfur via oxidation of SO_2 to SO_3 and subsequent hydration, in the exhaust plume, of SO_3 to H_2SO_4 The fuel sulfur content is the only factor that affects both emissions; flight altitude and engine power settings have no effect [22], [37], [38].

The EIs of SO_2 and Sulfate are calculated from the formula given in[22], [37] as:

$$EI_{SO_2}\left(\frac{mg}{kg}\right) = 10^6\left[\frac{FSC\cdot(1-\varepsilon)\cdot MW_{SO_2}}{MW_{Sulphur}}\right]\cdot S_r , \quad (21)$$

$$EI_{sulfate}\left(\frac{mg}{kg}\right) = 10^6\left[\frac{FSC\cdot\varepsilon\cdot MW_{SO_4^{2-}}}{MW_{Sulphur}}\right]\cdot S_r . \quad (22)$$

where MW_{SO_2} is the molecular weight of the SO_2 equal to 64, $MW_{sulfate}$ is the molecular weight of the SO_4^{2-} equal to 96, MW_{Sulfur} is the molecular weight of elemental sulfur equal to 32, FSC is fuel sulfur content (mass fraction), ε is fuel sulfur conversion efficiency (mass fraction, e.g., 0.02) with a median value of 2.4, and S_r is the unit scale factor equal to 1 mg/kg. Since the EIs of SO_2 and sulfate only depend on the sulfur content of the fuel, Equations 19 and 20 can be used for both kerosene fuels and kerosene-SAF blends. The sulfur content of each neat fuel component can be used in the same way as the computation of hydrogen and LHV of blends to get the sulfur content of the kerosene-SAF blend:

$$FSC_{blend} = \sum_i w_i \cdot FSC_i \quad , \tag{23}$$

where FSC_{blend} is the sulfur content of the blend, w_i is the weight fraction of the neat blend component, and FSC_i is the sulfur content of the neat blend component. Now, it is possible to calculate EIs for SO_2 and sulfate for kerosene-SAF blends by replacing the *FSC* in Equations 19 and 20 with FSC_{blend}.

4.5 Assessment of climate effects when burning SAF

The examples presented in Section 3 regarding the climate impact of aviation were based on conventional kerosene fuel. The Patterns of aCCFs, except for contrails, are still valid as they were independent of emissions. For instance, in the case of aCCF of NO_x emissions, the unit is K/kg(NO_2). Therefore, based on the fuel type, one can calculate the corresponding climate impact in temperature change by multiplying the aCCF by NO_x emissions for a given flight profile. The aCCF of contrails has been specifically developed for the kerosene fuel. Therefore, it cannot be adopted to assess the climate impact of contrails when burning SAF [10].

The gridded CoCiP model is employed to evaluate the climate impact of contrails from SAF. The gridded CoCiP, based on the emissions of relevant species and meteorological conditions, performs simulations to calculate the properties (e.g., optical depth) and lifecycle of contrails and, finally, the corresponding climate impact. Therefore, by adjusting for emissions from SAF using the methodologies proposed in this section, we can estimate the climate effects associated with contrails using the gridded CoCiP model.

The most relevant emissions required for gridded CoCiP are the water vapor and nvPM number emissions, which depend on the thrust settings, fuel hydrogen, and aromatic content. As can be understood from the formulations given in Section 4, using SAF increases the hydrogen content and LHV, leading to a reduction in nvPM compared to conventional kerosene fuel. Reduction in nvPM can result in a significant decrease in the initial contrail ice crystal number and optical depth while increasing the ice crystal size as validated through in situ measurements [6]. These changes are expected to reduce the contrail lifetime and climate forcing. It should be noted that while burning SAF is beneficial in terms of reducing lifetime and climate impact, it can increase contrail occurrence due to increased water vapor emissions (as the hydrogen content of the fuel increases for SAF).

In Figure 10, based on gridded CoCiP, we have generated a climate sensitivity map for contrails using conventional kerosene fuel, SAF, and a blend of SAF with kerosene at a 50% ratio. It is clear from the maps that fueling aircraft with SAF will reduce the lifetime of contrails and, as a result, reduce its impact on climate change (i.e., warming/cooling), in line with what has been observed within in situ measurements. It should be noted that the calculation of emissions, particularly for SAF, is ongoing research within the project. Therefore, the assessments provided

here may change as more sophisticated methods for calculating emissions are developed throughout this project.

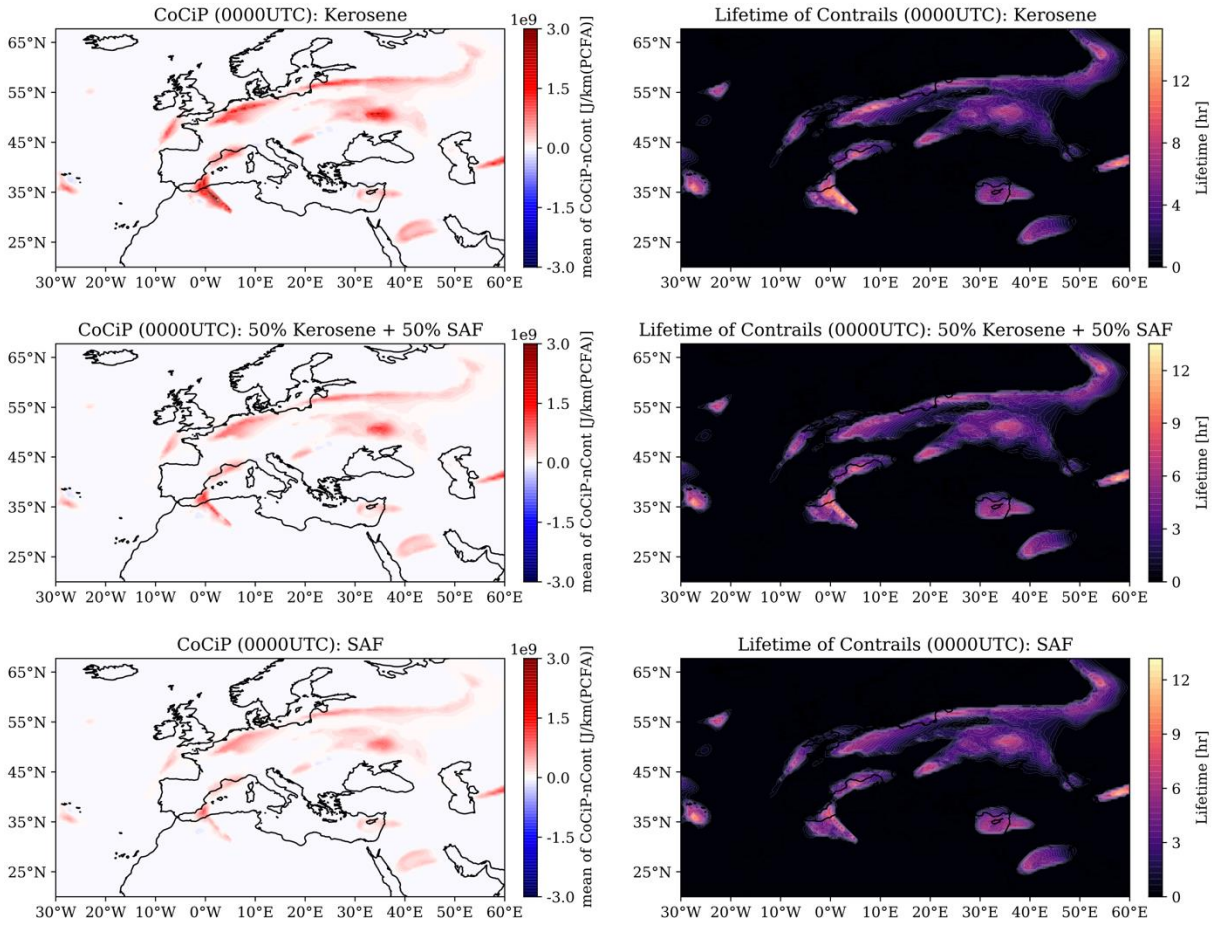

Figure 10. Lifetime and energy forcing of contrails estimated using gridded CoCiP for kerosene fuel, pure SAF, and SAF blended with kerosene with 50% blending ratio on 1st of January 2023, over European airspace at 250hPa.

5 Robust Climate Change Models

The assessment of climate effects is very challenging as it is a very complex multi-disciplinary topic, including estimation of aircraft emissions, weather forecast and representation of background conditions in numerical models, and climate science (e.g., chemical transformations, microphysics, radiation) (Matthes et al. 2023). Therefore, high uncertainty is expected in estimating the climate effects induced by aviation, as pointed out by Lee et al. (2021) [3]. Such potential uncertainty needs to be carefully considered when planning aircraft trajectories [14]. Indeed, deviating from business-as-usual routes for the benefit of climate has some side effects on the

ATM system in terms of operational cost [39] and stability [40]. Therefore, we need to be more confident about the mitigation that can be achieved by re-routing aircraft trajectories. This calls for robust climate change functions and, consequently, robust flight planning, considering different sources of uncertainty affecting the estimation of climate effects. In order to address potential uncertainties when planning flights in a climate-friendly manner, we first need to identify and quantify them.

Looking at the estimations reported by Lee et al., 2021 [3], it can be understood that a large part of the uncertainties in estimating climate impact is due to variations in model results from different calculation methods, such as different chemistry or cloud schemes [3]. This implies that the confidence level of climate impact estimations can be improved by having consistent assessments from all potential estimates. In the context of climate-optimal flight planning, we interpret such uncertainty as the mismatch between climate-sensitive areas identified with different climate impact assessment approaches, emission calculation methods, and weather data. One direction of study to increase the reliability of the climate impact assessment is, therefore, to perform further research to better understand and quantify aviation-induced climate effects in order to identify and resolve discrepancies between available impact estimates, as climate impact estimates with different approaches should ideally provide consistent measurements. The other direction, which we aim to introduce and explore in this project, is to consider all possible estimations of climate effects in flight planning in order to increase the confidence level of solutions by flying in areas with a good level of agreement with all potential estimates.

In the following, we will present the main sources that induce uncertainty in climate impact estimates. These uncertainty effects will be accounted for in order to deliver robust climate change functions. By robustness, we refer to a concept similar to an ensemble weather forecast, i.e., adding another dimension (called member) to 4D (i.e., time, flight level, latitude, and longitude) datasets of climate impact estimates, leading to a 5D dataset: member, time, flight level, latitude, and longitude. Such a data structure is compatible with the robust aircraft trajectory optimization tools developed in WP3 (Task 3.3). The aim is to provide flight planning tools with all potential climate impact estimates to determine climate-optimized trajectories with minimal sensitivity to climate impact assessment uncertainty.

5.1 Weather forecast uncertainty

The non-CO_2 climate effects of aviation strongly rely on weather conditions. Since the required meteorological variables are obtained from standard weather forecasts, they are inevitably uncertain. This, in turn, can lead to increased uncertainty in the climate estimates and, therefore, inefficiency of planned aircraft trajectories. Here, we analyze how we can generally quantify the impact of meteorological uncertainty on climate impact estimates. For this, we need weather data that includes uncertainty quantification. In this project, the forecast-related uncertainties will be characterized by employing ensemble prediction system (EPS) weather forecasts, a numerical weather prediction method introduced to deal with uncertainty in the weather

forecast. These are forecasts in which both the initial conditions and the physical parameters of a numerical weather integration model are slightly modified from one member to another and provide N_{EPS} (typically N_{EPS}=50) different predictions known as ensemble members. Each member of an ensemble represents one possible realization of meteorological situations. As the aCCFs take as inputs some meteorological variables, N_{EPS} different aCCFs can be calculated for an EPS weather forecast. For instance, the meteorological variables temperature and relative humidity over ice are required for the aCCF of nighttime contrails. Notice that relative humidity over ice is required for identifying ice-supersaturated areas. Feeding N_{EPS} probable realizations of these meteorological variables (i.e., ensemble members), N_{EPS} different aCCFs (i.e., $aCCF_{Cont,i}$ for i=1, ⋯ , N_{EPS}) are calculated. The same applies to aCCFs of other species and the NO_X emission index (due to the dependency on ambient temperature and specific humidity).

To investigate the degree of uncertainty (or variability) in the meteorological variables provided by an EPS and its effects on the computed aCCFs, we take the standard deviation (SD) from 10 ensemble members of weather data obtained using the ERA5 reanalysis data products[5]. It should be noted that the reanalysis data products are generated from post- processing with observations. Thus, the variability among the ensemble members is expected to be lower than the forecast data with more ensemble members yet still valid to illustrate.

[5] https://cds.climate. copernicus.eu/

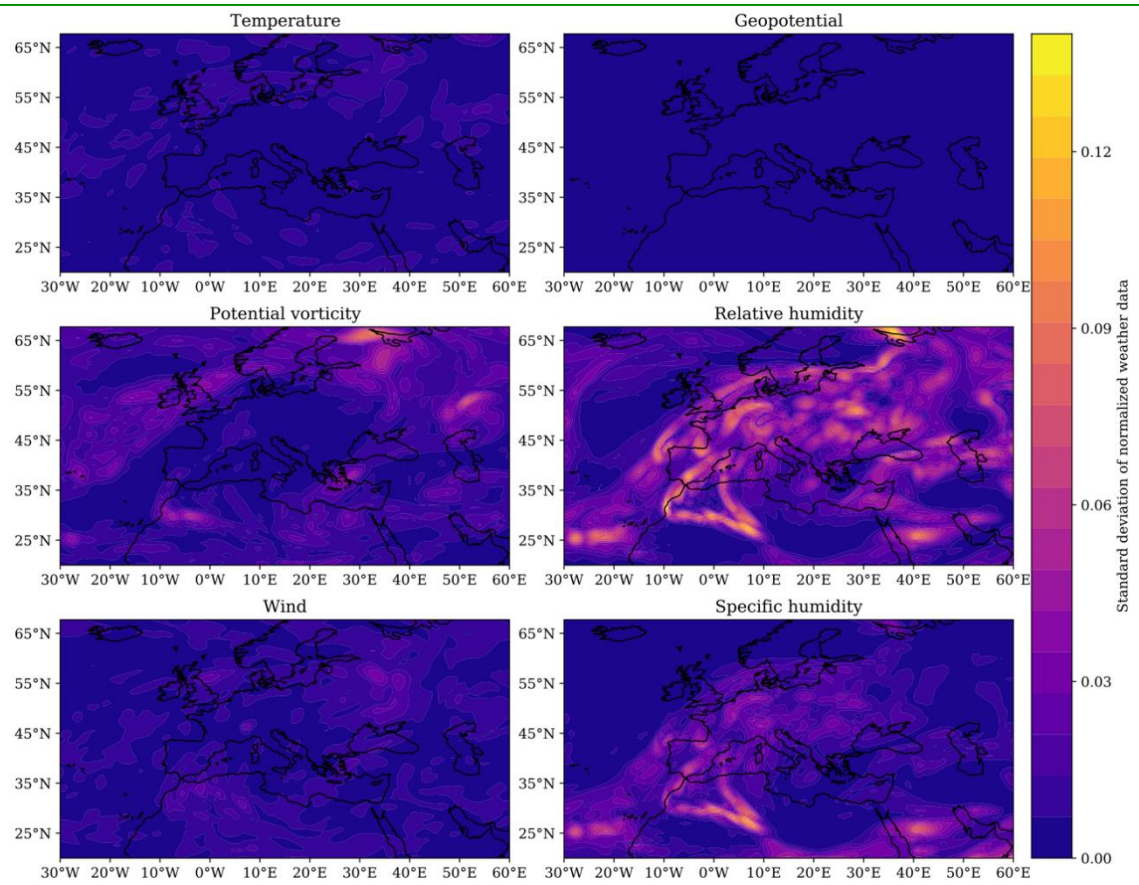

Figure 11. Variability (quantified using STD) of the meteorological conditions for an ensemble weather forecast with 10 ensemble members on 1st of January 2023, over European airspace at 250hPa.

Figure 11 shows the SD of weather variables required to calculate the aCCFs and predict aircraft trajectory on 1st of January 2023 at 250hPa. The SD is taken over the normalized variables (with respect to their maximum values) for comparison purposes. The variability of geopotential, temperature, and wind is small compared to potential vorticity, outgoing longwave radiation, and relative humidity. The SDs of the calculated aCCFs based on the ensemble members are illustrated in Figure 12. Since the aCCF of NO_x emissions (i.e., methane and ozone) depends on geopotential and temperature, its SD is small compared to the aCCFs of water vapor and nighttime contrails, which are based on potential vorticity and relative humidity (when applying the ice-supersaturated condition), respectively. Notice that the uncertainty in the climate impact of contrails is much higher than water vapor due to the variability of relative humidity in satisfying the persistency condition of contrails (see SD of PCFA in Figure 12). In spite of negligible uncertainty in the aCCF of NO_x and also relatively low uncertainty in the aCCF of water vapor compared to aCCF of contrails, due to the dominant climate impact of contrails, the net non-CO_2 climate effect is considerably uncertain (see SD of the merged aCCFs in Figure 12), which

must be crucially taken into consideration when planning climate-optimized trajectories.

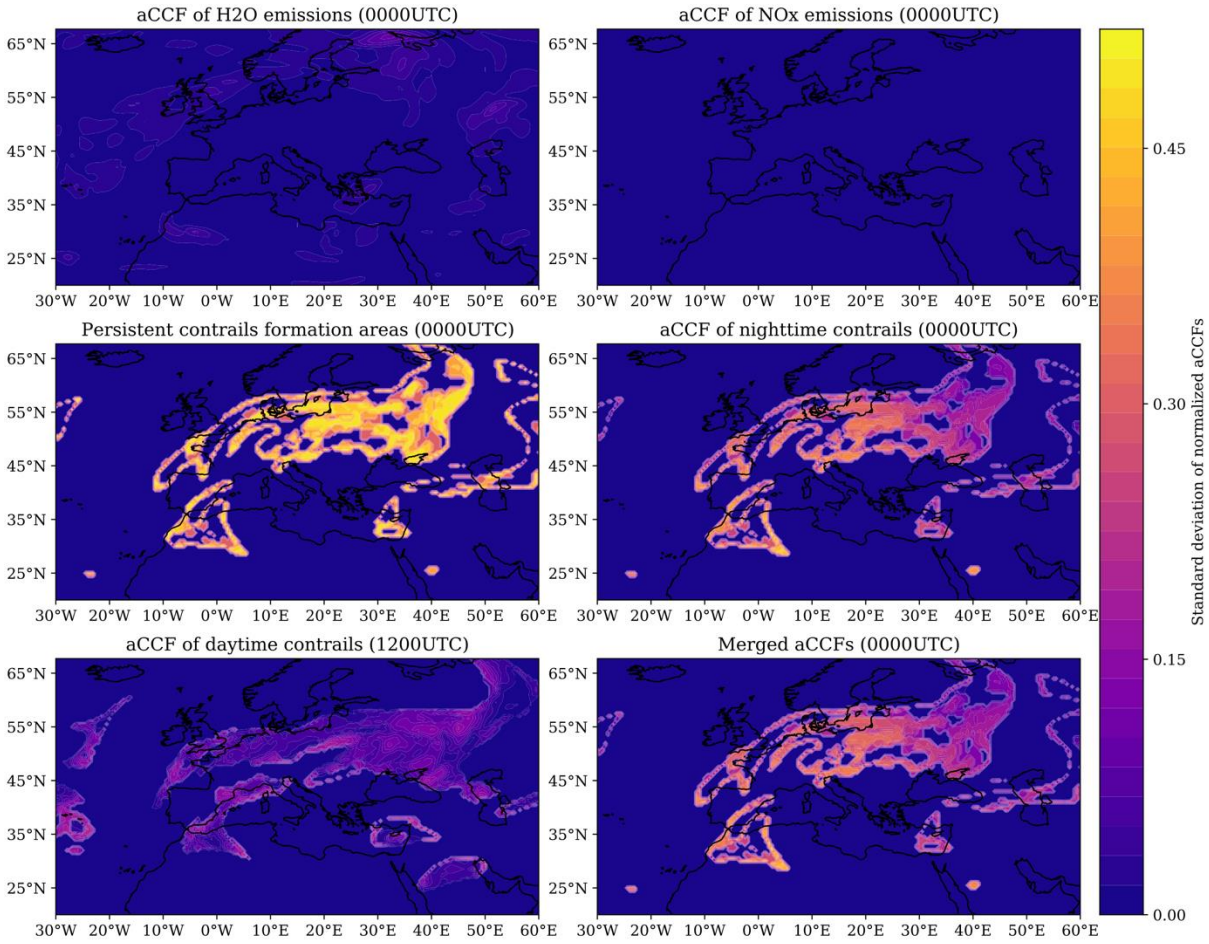

Figure 12. Variability (quantified using STD) of aCCFs for an ensemble weather forecast with 10 ensemble members on 1st of January 2023, over European airspace at 250hPa.

A similar conclusion can also be made when estimating climate sensitivity with gridded CoCiP. The standard deviation of contrails lifetime and climate impact in energy forcing using CoCiP is depicted in Figure 13. Due to reliance on highly uncertain meteorological variables such as outgoing longwave radiation and specific humidity, the resulting estimates are relatively uncertain.

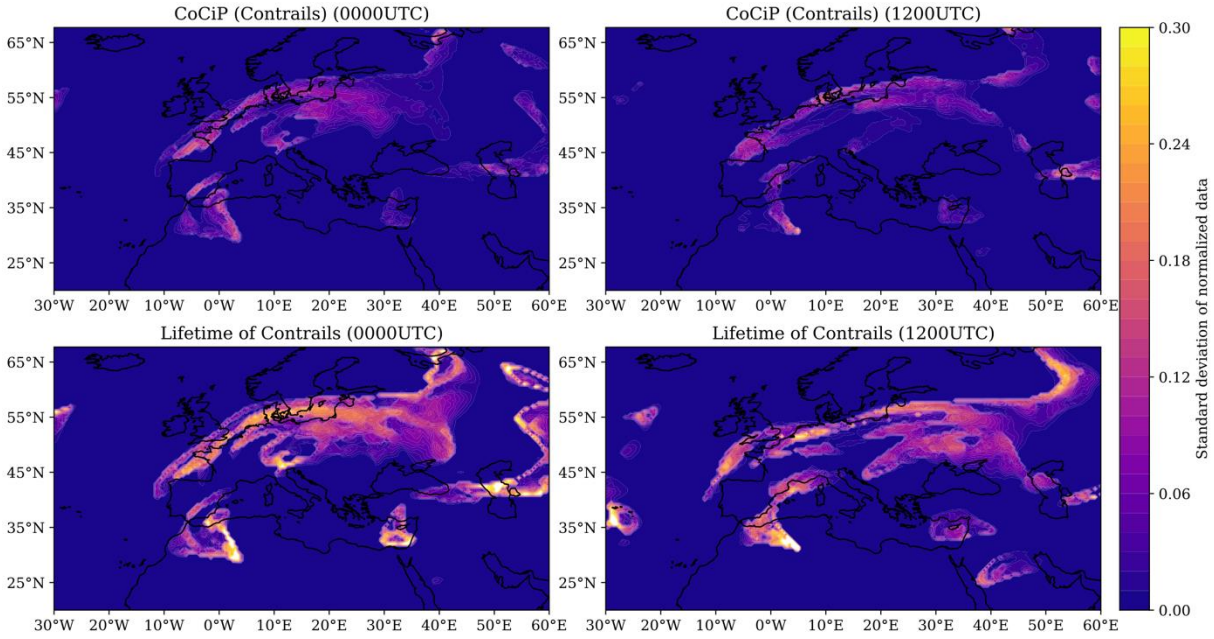

Figure 13. Variability (quantified using STD) of lifetime and energy forcing estimated using gridded CoCiP for an ensemble weather forecast with 10 ensemble members on 1st of January 2023, over European airspace at 250hPa.

All in all, the uncertainty in standard weather forecasts directly affects the climate impact prediction. The climate change functions that will be inputted to WP3, Task 3.3, include the impact of meteorological uncertainty.

5.1 Relative humidity correction

For contrail persistence, the ambient air needs to be supersaturated with respect to ice (relative humidity over ice > 100%). As already illustrated, strong variability in the relative humidity field is evident in ensemble simulations. Several studies reported an underprediction of the degree of ice supersaturation in numerical weather models (using, e.g., ERA-5 reanalysis data) due to the problematic forecast of relative humidity fields in the upper troposphere and lower stratosphere (UTLS) (e.g., see Gierens et al. (2020)). In particular, numerical weather prediction models are weakly supersaturated (RHi < 100%) and underestimate regions with very high supersaturations (RHi > 120%). Therefore, correction of relative humidity field is

required. In this project, the relative humidity field will be corrected using different approaches and in-situ measurements, e.g., from the In-service Aircraft for a Global Observing System (IAGOS) database (https://doi.org/10.25326/20, 2020) (see Teoh et al. (2022)). In order to explore the effects of relative humidity correction on the results, the contrails climate impact is assessed using CoCiP for corrected (with respect to IAGOS data) and uncorrected relative humidity fields, which is illustrated in Figure 14. A large difference can be seen between assessments, implying the necessity of improving the prediction of humidity field within numerical weather prediction models. In this project, different correction schemes will be proposed and considered within the trajectory optimization tool as other potential estimates.

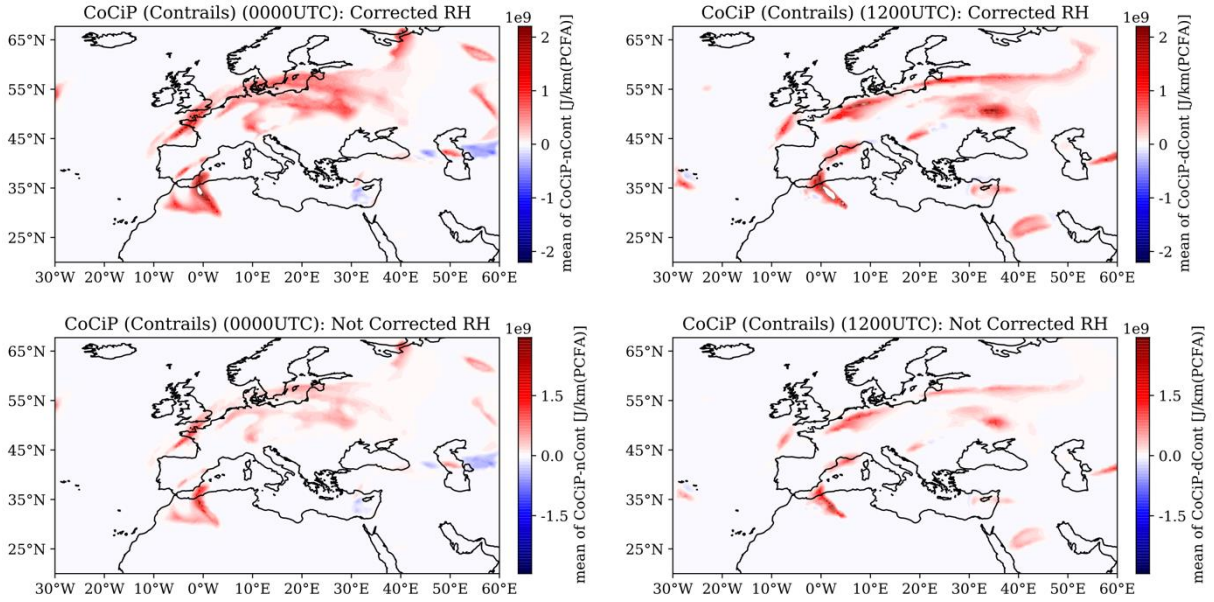

Figure 14. Comparison of contrails' climate impact using gridded CoCiP for corrected and uncorrected relative humidity fields on 1st of January 2023, over European airspace at 250hPa.

5.2 Climate impact modeling uncertainty

Several approaches have been published to quantify the climate effects of non-CO_2 species (see [5], Section 3). The difference between these approaches can be attributed to the required inputs and/or models themselves. The inputs are generally linked to meteorology (e.g., source of weather forecast and resolution) and emissions (e.g., DLR method [41] and Boeing Fuel Flow Method 2 [42]) as already presented. Parameters representing the model (e.g., forcing efficacy [3]), modeling approach (e.g., contrails aCCF and CoCiP), assumptions (e.g., contrail properties and lifetime in terms of contrails impact), and the physical climate metric (e.g., ATR, energy

forcing [11], global warming potential [43]) are some factors introducing uncertainty to the model. Such variations can lead to different estimates of climate effects. As presented in this report, the uncertainty in contrails' climate impact is relatively higher than that of other species. Currently, there are only two models capable of representing spatiotemporal dependency of contrails climate impact in the literature: aCCFs and gridded CoCiP. A comparison between aCCF and gridded CoCiP can be seen in Table 1, showing differences in the approach, required meteorological variables, and climate metric. Figure 11 depicts the contrails climate impact assessments using aCCF and gridded CoCiP on 1st of January 2023 over Europe. A significant discrepancy (e.g., cooling/warming, and location where persistent contrails are expected to from) can be observed in estimating climate impact in particular areas with these two approaches. Therefore, the climate impact modeling approach acts as another source of uncertainty that we aim to account for.

	aCCF	Gridded CoCiP
Species	Contrails, Ozone, Methane, PMO, Water Vapor, CO_2	Only Contrails
Modeling approach	Comprehensive Lagrangian simulations in a climate chemistry model, approximated with mathematical formula (i.e., aCCFs) correlating local atmospheric fields with the simulations results.	Lagrangian plume model applied to small generic flight segments in each 4D grid cell
Climate metric	Average Temperature Response of the Planet at 20, 50, 100 Years	Energy Forcing
Validity	aCCF-V1.0a: North Atlantic flight corridor, specific summer and winter weather patterns	Globally, and not restricted to specific weather-patterns
Tool	Python library CLIMaCCF	Python library pycontrails
Input	MET variables at the time of emissions	MET variables at various time steps
Met variables	Geopotential, OLR, temperature, potential vorticity, relative humidity	Wind, specific humidity, ice water content, temperature, radiations

Table 1. Comparison of aCCFs and gridded CoCiP.

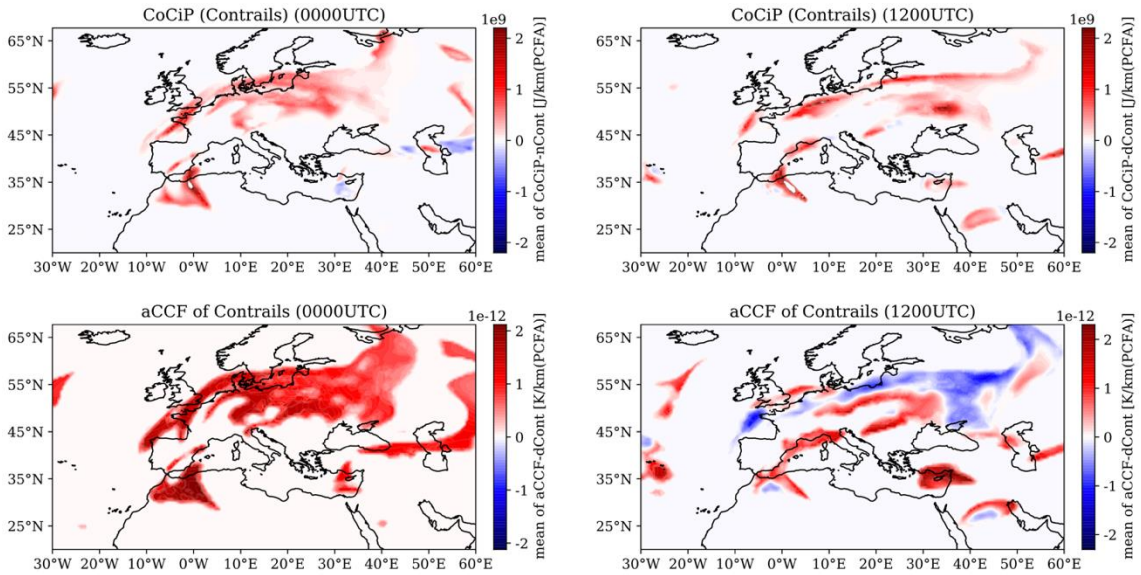

Figure 15. Comparison of contrails' climate impact estimated using aCCF and gridded CoCiP on 1st of January 2023, over European airspace at 250hPa.

6 Conclusions

In order to mitigate the non-CO_2 climate effects induced by aviation through flight planning, it is essential to develop mathematical models that provide detailed spatiotemporal information on the climate impact of non-CO_2 emissions. These climate effects include nitrogen oxides (NOx), water vapor, and contrail-cirrus. The primary goal of this deliverable is to provide robust climate change functions for aircraft emissions when burning conventional kerosene fuel, SAF, and various blends of SAF with kerosene. These functions, calculated from meteorological weather forecast data, offer advanced meteorological (MET) services for climate-optimized flight planning, informing airspace users about the environmental impact of aviation emissions at specific locations.

In Section 3, we presented two state-of-the-art approaches to provide spatiotemporal information on climate sensitivity, specifically developed for conventional kerosene fuel: aCCF and the gridded CoCiP. We conducted a regional analysis of aCCFs for individual species and their combined effect, focusing on Europe. This analysis revealed that the climate impact of contrails is more significant than that of other species. Persistent contrails are primarily formed in ice-supersaturated regions. Therefore, slight deviations in flight paths to avoid these areas can significantly reduce climate impact

To estimate the climate impact in temperature change or energy forcing, aircraft emissions, or the distance flown in areas prone to persistent contrail formation in terms of contrails climate impact are needed. Section 4 discussed our methods for calculating emissions from kerosene fuel and the necessary adjustments for SAF. The proposed approach for computing SAF emissions enabled the adaptation of climate impact assessments for SAF and its blends with kerosene. We compared the climate impact of contrails using gridded CoCiP for pure kerosene, 100% SAF, and a 50% SAF-kerosene blend. Our findings indicated that using SAF can reduce the lifetime of contrails and, consequently, their associated energy forcing.

The assessment of climate effects is very challenging as it is a complex multi-disciplinary topic that is associated with high uncertainty. In Section 5, we identified various sources that introduce uncertainty to the climate estimate, including aircraft emissions calculation, weather forecasts, identification of ice-supersaturated areas, and complexities in climate science (e.g., chemical transformations, microphysics, radiation) in order to deliver climate change functions containing uncertainty effects. The proposed climate change functions with uncertainty quantification, referred to as robust climate change functions, are compatible with robust aircraft trajectory optimizers developed in WP3, aimed at determining climate-optimized flight paths with minimal sensitivity to identified uncertainties.

In conclusion, the solution proposed in this deliverable enhances situational awareness of airspace users regarding climate impacts by providing spatially and temporally resolved information on climate sensitivity for both kerosene fuel and SAF, including potential uncertainty effects. Additionally, our solution aids in assessing and optimizing the environmental performance of aircraft operations, with a particular focus on the effects of CO_2, NO_x, H_2O, and contrail cirrus.

References

[1] Eurocontrol, “EUROCONTROL Aviation Outlook 2050.” 2022. [Online]. Available: https://www.eurocontrol.int/publication/eurocontrol-aviation-outlook-2050

[2] International Air Transport Association (IATA), “Air passenger numbers to recover in 2024.” 2022. [Online]. Available: https://www.iata.org/en/pressroom/2022-releases/2022-03-01-01/

[3] D. S. Lee *et al.*, “The contribution of global aviation to anthropogenic climate forcing for 2000 to 2018,” *Atmos Environ*, vol. 244, p. 117834, 2021.

[4] J. van Manen and V. Grewe, “Algorithmic climate change functions for the use in eco-efficient flight planning,” *Transp Res D Transp Environ*, vol. 67, pp. 388–405, 2019.

[5] A. Simorgh *et al.*, “A Comprehensive Survey on Climate Optimal Aircraft Trajectory Planning,” *Aerospace*, vol. 9, no. 3, 2022, doi: 10.3390/aerospace9030146.

[6] C. Voigt *et al.*, “Cleaner burning aviation fuels can reduce contrail cloudiness,” *Commun Earth Environ*, vol. 2, no. 1, p. 114, 2021, doi: 10.1038/s43247-021-00174-y.

[7] L. Dray *et al.*, “Cost and emissions pathways towards net-zero climate impacts in aviation,” *Nat Clim Chang*, vol. 12, no. 10, pp. 956–962, 2022, doi: 10.1038/s41558-022-01485-4.

[8] R. Teoh *et al.*, “Targeted use of sustainable aviation fuel to maximize climate benefits,” *Environ Sci Technol*, vol. 56, no. 23, pp. 17246–17255, 2022.

[9] S. Dietmüller *et al.*, “A Python library for computing individual and merged non-CO_2 algorithmic climate change functions: CLIMaCCF V1. 0,” *Geosci Model Dev*, vol. 16, no. 15, pp. 4405–4425, 2023.

[10] F. Yin *et al.*, “Predicting the climate impact of aviation for en-route emissions: the algorithmic climate change function submodel ACCF 1.0 of EMAC 2.53,” *Geosci Model Dev*, vol. 16, no. 11, pp. 3313–3334, 2023.

[11] U. Schumann, “A contrail cirrus prediction model,” *Geosci Model Dev*, vol. 5, no. 3, pp. 543–580, 2012.

[12] H. Appleman, “The formation of exhaust condensation trails by jet aircraft,” *Bull Am Meteorol Soc*, vol. 34, no. 1, pp. 14–20, 1953.

[13] V. Grewe and K. Dahlmann, “How ambiguous are climate metrics? And are we prepared to assess and compare the climate impact of new air traffic technologies?,” *Atmos Environ*, vol. 106, pp. 373–374, 2015.

[14] K. Dahlmann, V. Grewe, C. Frömming, and U. Burkhardt, “Can we reliably assess climate mitigation options for air traffic scenarios despite large uncertainties in atmospheric processes?,” *Transp Res D Transp Environ*, vol. 46, pp. 40–55, 2016.

[15] M. Ponater, S. Pechtl, R. Sausen, U. Schumann, and G. H"uttig, “Potential of the cryoplane technology to reduce aircraft climate impact: A state-of-the-art assessment,” *Atmos Environ*, vol. 40, no. 36, pp. 6928–6944, 2006.

[16] A. Rap, P. M. Forster, J. M. Haywood, A. Jones, and O. Boucher, “Estimating the climate impact of linear contrails using the UK Met Office climate model,” *Geophys Res Lett*, vol. 37, no. 20, 2010.

[17] M. Bickel, M. Ponater, L. Bock, U. Burkhardt, and S. Reineke, “Estimating the effective radiative forcing of contrail cirrus,” *J Clim*, vol. 33, no. 5, pp. 1991–2005, 2020.

[18] B. Graver and D. Rutherford, “Transatlantic airline fuel efficiency ranking, 2017,” *International Council on Clean Transportation*, 2018.

[19] J. E. Penner, D. Lister, D. J. Griggs, D. J. Dokken, and M. McFarland, “Aviation and the global atmosphere: a special report of the Intergovernmental Panel on Climate Change,” 1999.

[20] M. Shapiro *et al.*, “Forecasting Contrail Climate Forcing for Flight Planning and Air Traffic Management Applications,” in *The 5th International Conference on Transport, Atmosphere and Climate (TAC)*, 2022.

[21] Arthur H. Lefebvre and D. R. Ballal, *Gas Turbine Combustion Alternative fuels and emissions*, 3rd ed. 2010.

[22] M. Masiol and R. M. Harrison, “Aircraft engine exhaust emissions and other airport-related contributions to ambient air pollution: A review,” *Atmos Environ*, vol. 95, pp. 409–455, 2014, doi: 10.1016/J.ATMOSENV.2014.05.070.

[23] D. DuBois and G. C. Paynter, “Fuel Flow Method2 for Estimating Aircraft Emissions,” 2006.

[24] D. Ahrens, Y. Méry, A. Guénard, and R. C. Miake-Lye, “A New Approach to Estimate Particulate Matter Emissions From Ground Certification Data: The nvPM Mission Emissions Estimation Methodology,” *J Eng Gas Turbine Power*, vol. 145, no. 3, pp. 1–12, Mar. 2023, doi: 10.1115/1.4055477.

[25] R. Fusaro, N. Viola, and D. Galassini, “Sustainable Supersonic Fuel Flow Method: An Evolution of the Boeing Fuel Flow Method for Supersonic Aircraft Using Sustainable Aviation Fuels,” *Aerospace*, vol. 8, no. 11, p. 331, Nov. 2021, doi: 10.3390/aerospace8110331.

[26] A. Zschocke, S. Scheuermann, and J. Ortner, “High Biofuel Blends in Aviation (HBBA),” 2017.

[27] R. Striebich, L. Shafer, M. J. DeWitt, Z. West, T. Edwards, and W. Harisson, “Dependence of Fuel Properties During Blending of Iso-Paraffinic Kerosene and Petroleum-Derived Jet Fuel,” 2008.

[28] E. Corporan *et al.*, “Impacts of fuel properties on combustor performance, operability, and emissions characteristics,” *AIAA SciTech Forum - 55th AIAA Aerospace Sciences Meeting*, no. January, pp. 1–19, 2017, doi: 10.2514/6.2017-0380.

[29] A. J. Beyersdorf *et al.*, “Reductions in aircraft particulate emissions due to the use of Fischer–Tropsch fuels,” *Atmos Chem Phys*, vol. 14, no. 1, pp. 11–23, Jan. 2014, doi: 10.5194/acp-14-11-2014.

[30] A. Agarwal *et al.*, “SCOPE11 Method for Estimating Aircraft Black Carbon Mass and Particle Number Emissions,” *Environ Sci Technol*, vol. 53, no. 3, pp. 1364–1373, 2019, doi: 10.1021/acs.est.8b04060.

[31] R. Teoh *et al.*, “Targeted Use of Sustainable Aviation Fuel to Maximize Climate Benefits,” *Environ Sci Technol*, vol. 56, no. 23, pp. 17246–17255, 2022, doi: 10.1021/acs.est.2c05781.

[32] D. Bulzan *et al.*, “Gaseous and Particulate Emissions Results of the NASA Alternative Aviation Fuel Experiment (AAFEX),” in *Volume 2: Combustion, Fuels and Emissions, Parts A and B*, ASMEDC, Oct. 2010, pp. 1195–1207. doi: 10.1115/GT2010-23524.

[33] M. T. Timko *et al.*, “Combustion Products of Petroleum Jet Fuel, a Fischer–Tropsch Synthetic Fuel, and a Biomass Fatty Acid Methyl Ester Fuel for a Gas Turbine Engine,” *Combustion Science and Technology*, vol. 183, no. 10, pp. 1039–1068, Oct. 2011, doi: 10.1080/00102202.2011.581717.

[34] O. J. Hadaller and J. M. Johnson, “World Fuel Sampling Program. Final Report.CRC Report No. 647,” 2006.

[35] D. Bell, J. S. Heyne, S. H. Won, F. Dryer, F. M. Haas, and S. Dooley, “On the Development of General Surrogate Composition Calculations for Chemical and Physical Properties,” in *55th AIAA Aerospace Sciences Meeting*, Reston, Virginia: American Institute of Aeronautics and Astronautics, Jan. 2017, pp. 1–13. doi: 10.2514/6.2017-0609.

[36] P. Vozka, D. Vrtiška, P. Šimáček, and G. Kilaz, “Impact of Alternative Fuel Blending Components on Fuel Composition and Properties in Blends with Jet A,” *Energy and Fuels*, vol. 33, no. 4, pp. 3275–3289, 2019, doi: 10.1021/acs.energyfuels.9b00105.

[37] International Civil Aviation Organization (ICAO), *Doc 9889 - Airport air quality manual. Second Edition*, Second. 2020.

[38] D. E. Hunton *et al.*, “Chemical ionization mass spectrometric measurements of SO2 emissions from jet engines in flight and test chamber operations,” *Journal of Geophysical Research Atmospheres*, vol. 105, no. D22, pp. 26841–26855, 2000, doi: 10.1029/2000JD900383.

[39] M. Niklaß, V. Grewe, V. Gollnick, and K. Dahlmann, “Concept of climate-charged airspaces: a potential policy instrument for internalizing aviation’s climate impact of non-CO2 effects,” *Climate Policy*, vol. 21, no. 8, pp. 1066–1085, 2021.

[40] F. Baneshi, M. Soler, and A. Simorgh, “Conflict assessment and resolution of climate-optimal aircraft trajectories at network scale,” *Transp Res D Transp Environ*, vol. 115, p. 103592, 2023.

[41] F. Deidewig, A. Döpelheuer, and M. Lecht, “Methods to assess aircraft engine emissions in flight,” in *ICAS PROCEEDINGS*, 1996, pp. 131–141.

[42] D. DuBois and G. C. Paynter, “‘Fuel Flow Method 2’ for Estimating Aircraft Emissions,” *SAE Transactions*, pp. 1–14, 2006.

[43] A. Vitali, M. Battipede, and A. Lerro, “Multi-Objective and Multi-Phase 4D Trajectory Optimization for Climate Mitigation-Oriented Flight Planning,” *Aerospace*, vol. 8, no. 12, p. 395, 2021.